[Supplementary material]

The power of relics: radiocarbon and histo-taphonomic evidence for the curation and excarnation of human remains in Bronze Age Britain

Thomas J. Booth[1,*] & Joanna Brück[2]

[1] *Francis Crick Institute, London, UK*

[2] *School of Archaeology, University College Dublin, Ireland*

[*] *Author for correspondence:* ✉ *thomas.booth@crick.ac.uk*

Section 1. Chronological models.

This section provides details of the chronological models we developed in OxCal 4.3 using the IntCal13 curve to produce the calculations discussed in the main paper (Bronk Ramsey 2009a; Reimer *et al*. 2013). Table S1 includes all of the radiocarbon dates we used in our analyses. Table S2 contains tables for all of the outputs and agreement indices generated by combine functions and chronological models discussed below. Table S3 contains a summary of these results, calculations of Offsets between radiocarbon determinations and summaries of modelled and unmodeled Differences calculated in OxCal. Table S3 also includes details of the paired radiocarbon dates we compared to generate Offsets and Intervals in BChron. For each deposit we investigated we include here brief descriptions and, in cases where we used complex phase/sequence models, figures (including OxCal scripts) showing the approaches we used to test whether particular bones were likely to have been old when they were deposited. Testing usually made use of the Combine function in OxCal (where dated materials were associated in the same contexts) and/or phase models. The Combine function tries to produce a combined calibrated radiocarbon date distribution from two or more dates assuming that they relate to the same event. As part of this process OxCal performs a X^2 test to assess the probability that the dates are statistically consistent (i.e. at 95% confidence we cannot reject the null hypothesis that the dates relate to the same event). We also include similar details for models which we used to generate unmodeled and modelled Difference probability ranges, with the modelled Differences representing a scenario where human remains identified as possibly curated were assumed to have been old when they were deposited. The modelled Differences involve placing dates in a Sequence in OxCal, which generates new Difference probability distributions assuming that one of the dates is older than the other. These modelled differences are intended to provide more constrained

estimates of timescales over which human remains may have been curated. Agreement indices <60 for models were considered to be poor and >60 were considered to be good (Bronk Ramsey 2009b).

Out of 36 cases where we used the Combine function and performed X^2 tests, 13 (36 per cent) failed. We would expect that 5 per cent of X^2 tests to fail by chance (Bronk Ramsey 2009a). A one-tailed proportions test of our X^2 test results against an invented similar-sized sample where 5 per cent fail (i.e. n=36, 34 non-significant and 2 significant results) suggests that the rate of failure in our Bronze Age samples is significantly higher than what we would expect to find by chance ($z=3.1921$, $p<0.001$, Bonferroni p-value threshold = 0.013). It is difficult to define a threshold of statistical significance for all outcomes including those where we only have agreement indices. A one-tailed proportions test of our Bronze Age results against an invented, similar-sized sample with an arbitrary but conservative 20 per cent rate of anomalous results (i.e. 44 non-significant and 11 significant) indicates that there were significantly more anomalous results in our Bronze Age sample ($z=-2.4759$, $p=0.007$, Bonferroni p-value threshold = 0.013). Anomalous dates were detected through all phases of the Bronze Age.

We also produced similar distributions (Intervals) for differences between dates from human bones and associated material in the Bchron program. We summed all of our BChron Intervals in R by combining them as a vector (Haslett & Parnell 2008; R Core Team 2013). We tested whether our combined Bronze Age Interval distribution was significantly lower than 0 (i.e. significantly early) by comparing it against a control sample consisting of a normal distribution with a mean of 0 and a similar standard deviation to our observed distribution (n=560,000, mean = 0, standard deviation = 178.2408), using a one-tailed Wilcoxon rank sum test (Figure 5). The result indicated that our summed Bronze Age Intervals were significantly older than the control ($W=1.183 \times 10^{11}$, $p<0.001$, Bonferroni p-value threshold = 0.013). This result provides further evidence in addition to the X^2 tests and chronological modelling for the presence of anomalously old human remains in our sample set and is consistent with curation of human bone through the Bronze Age.

We noticed that Bronze Age intervals which were not significantly anomalous were still slightly offset from a comparable control (normal distribution, n=340,000, mean = 0, standard deviation = 181.0332; Figure 6). Bronze Age human remains which were curated for decades or sometimes centuries would not always show up as anomalously old using the tests provided in OxCal (OSM Section 2). We performed another one-tailed Wilcoxon rank sum test of our combined Bronze Age intervals with all the anomalous intervals removed against

the control distribution described above. This Bronze Age distribution without anomalous dates was significantly older than the control ($W=5.0121 \times 10^{10}$, $p<0.001$, Bonferroni p-value threshold = 0.013), consistent with our hypothesis that this sample set likely includes curated human bones that do not show up in site-specific X^2 tests or agreement indices.

Boscombe Bowmen

The primary Boscombe Bowmen deposit consists of an articulated human skeleton from a wooden cist surrounded by the disarticulated human remains of at least three people (a juvenile and two adults), mainly consisting of crania and long bones (Fitzpatrick *et al*. 2011). We tested radiocarbon dates from the disarticulated bone representing different individuals against the accompanying articulated burial. We modified the model built in Fitzpatrick *et al*. (2011) to include the dates of the remains from the primary deposit in a Combine function to see whether they were likely to have died around the same time (Figures S1–S2). The Combine model showed poor agreement and failed the X^2 test because the date from 25010 was anomalously old (df=3 T=9.933(5% 7.8)). However, when we reran the model without the date from 25010 (OxA-13642), the Combine produced good model agreement indices, suggesting individuals represented by these bones could have died around the same time (Figures S3–S4). We calculated Differences in OxCal and Intervals in BChron by comparing the date from each disarticulated deposit against the date from the articulated burial (Figures S5–S6). For the modelled differences, the Sequence model was arranged with the assumption that the disarticulated bones were older than the articulated burial.

```
Plot()
 {
  Sequence("Boscombe_seq")
  {
   Boundary("Boscombe_start");
   Sequence("Sequence Grave")
   {
    Phase("Grave_fill")
    {
     Combine("Primary Burial")
     {
      R_Date("OxA-13542", 3955, 33);
      R_Date("OxA-13543", 3822, 33);
      R_Date("OxA-13681", 3825, 30);
      R_Date("OxA-13624", 3845, 27);
     };
                                    Sequence("Sequence_2")
     {
      R_Date("OxA-13598", 3889, 32);
      R_Date("OxA-13972", 3613, 28);
     };
    };
    R_Date("OxA-13599", 3681, 30);
                                                 };
   Boundary("Boscombe_end");
  };
 };
```

Figure S1. OxCal Script for the Boscombe Bowmen Phase model.

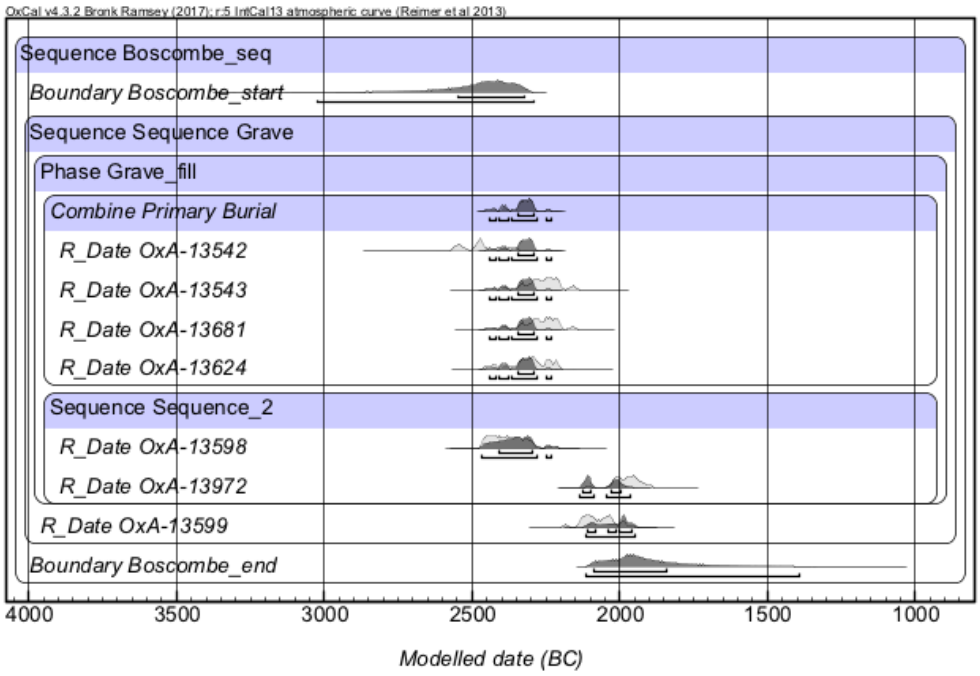

Figure S2. Boscombe Bowmen Phase model.

```
Plot()
 {
  Sequence("Boscombe_seq")
  {
   Boundary("Boscombe_start");
   Sequence("Sequence Grave")
   {
    Phase("Grave_fill")
    {
     Combine("Primary Burial")
     {
      R_Date("OxA-13543", 3822, 33);
      R_Date("OxA-13681", 3825, 30);
      R_Date("OxA-13624", 3845, 27);
     };
     Sequence("Sequence_2")
     {
      R_Date("OxA-13598", 3889, 32);
      R_Date("OxA-13972", 3613, 28);
     };
    };
    R_Date("OxA-13599", 3681, 30);
   };
   Boundary("Boscombe_end");
  };
 };
```

Figure S3. OxCal script for the Boscombe Bowmen Phase model with OxA-13642 removed.

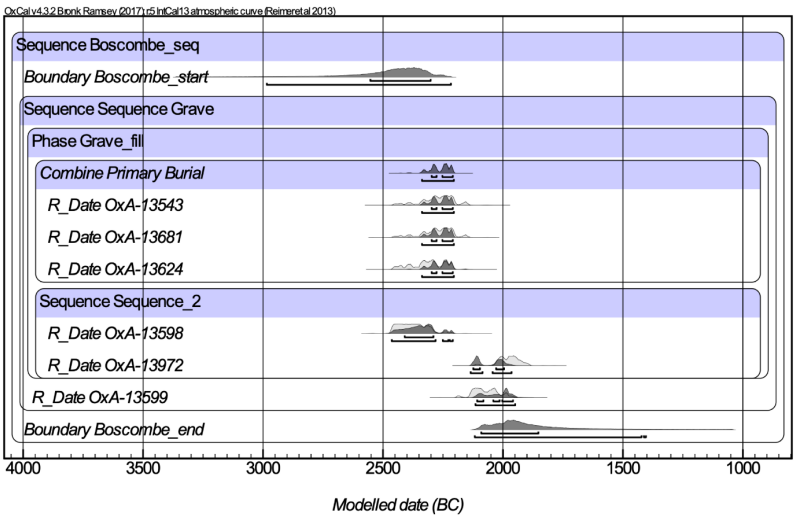

Figure S4. Boscombe Bowmen Phase model with OxA-13642 removed.

```
Plot()
 {
  Sequence("Boscombe_seq")
  {
   Boundary("Boscombe_start");
   Sequence("Sequence Grave")
   {
    Phase("Grave_fill")
    {
     Sequence("Sequence_1")
     {
      After("After_disarticulated")
      {
       R_Date("OxA-13542", 3955, 33);
       R_Date("OxA-13543", 3822, 33);
       R_Date("OxA-13681", 3825, 30);
      };
      R_Date("OxA-13624", 3845, 27);
     };
     Sequence("Sequence_2")
     {
      R_Date("OxA-13598", 3889, 32);
      R_Date("OxA-13972", 3613, 28);
     };
    };
    R_Date("OxA-13599", 3681, 30);
   };
   Boundary("Boscombe_end");
   Difference("Boscombe_25010_diff", "OxA-13542", "OxA-13624");
   Difference("Boscombe_25008_diff", "OxA-13543", "OxA-13624");
   Difference("Boscombe_25010b_diff", "OxA-13681", "OxA-13624");
  };
 };
```

Figure S5. OxCal script for Boscombe Bowmen Curation sequence.

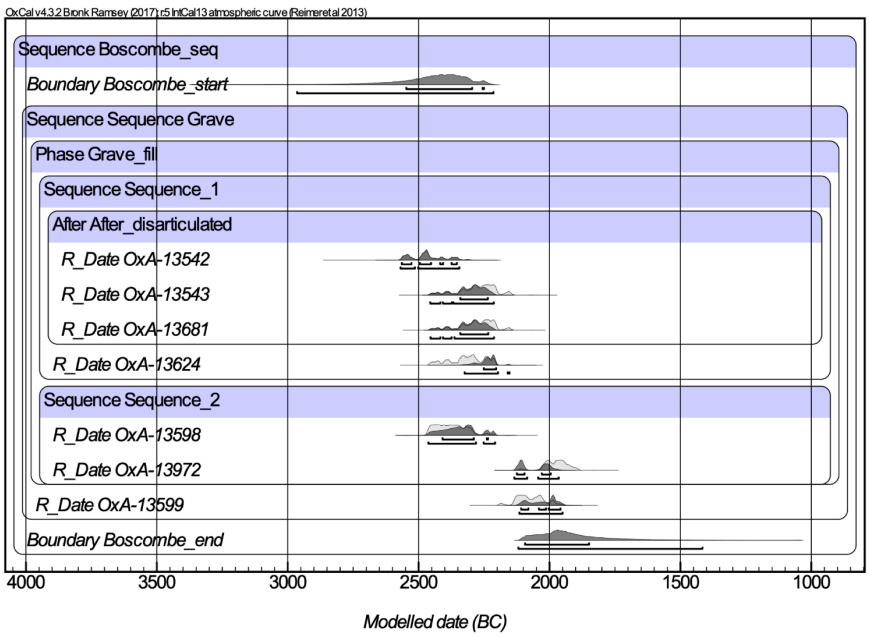

Figure S6. Boscombe Bowmen Curation sequence.

Bradley Fen F.1102

We obtained three radiocarbon dates on bones from Bradley Fen F.1102, a deposit in a pond surrounding a burnt mound (Gibson & Knight 2006). The bones consisted of a disarticulated human cranial fragment and two disarticulated faunal bones. Combination of these three dates using the Combine function in OxCal produced poor agreement indices. The BRAMS-1539 date was notably older than the other two and the ^{13}C value obtained from the AMS was notably enriched (Table S2). The early date of this sample might be due to a marine reservoir effect. We removed the BRAMS-1539 from the analysis and ran the Combine model again. This still produced poor agreement indices and failed the X^2 Test, as the disarticulated human bone was anomalously older than the disarticulated faunal bone. We calculated Differences in OxCal by comparing these two dates. Modelled Diffeerences were calculated by comparing dates in a Sequence model assuming that the disarticulated cranial fragment was older than the faunal bone. We did not calculate an Interval in BChron for this deposit, as the date of deposit based on the disarticulated faunal bone turned out to be Iron Age.

Bradley Fen 785

We obtained radiocarbon dates from a complete, articulated skeleton (Sk. 785, BRAMS-1691) that showed histological evidence for having been formerly mummified (Booth *et al*. 2015) as well as cortical modification indicative of scavenger modification, and an accompanying extra disarticulated human fibula (BRAMS-1690; Gibson & Knight 2006). Combination of these two dates using the Combine function in OxCal produced poor agreement indices and failed the X^2 test because the disarticulated human fibula was anomalously old. We calculated Differences in OxCal by comparing these two dates. The modelled Difference was generated by analysing the dates as a Sequence assuming the disarticulated fibula was older than the articulated skeleton. As radiocarbon date from the complete articulated skeleton suggested that this was an Iron Age deposit, we did not generate a BChron Interval.

Bradley Fen 853

We obtained radiocarbon dates from a complete articulated human skeleton that had been deposited headfirst in a watering hole, as well as a disarticulated cow bone and an articulated skeleton of a fox or dog from a spread of organic material covering this skeleton (Gibson & Knight 2006). Histological analysis of the human skeleton suggested that it may have been formerly mummified (Booth *et al*. 2015). Combination of all dates using the Combine

function in OxCal assuming that the dates referred to the same event produced poor agreement indices and failed the X^2 test (df=2 T=7.647(5% 6.0)). This was because the radiocarbon dates from the cow bone, rather than the human skeleton were anomalously old. It is possible that the cow bone was already old when it was deposited or the date was erroneous. We ran the Combine model again with just the dates from human burial and articulated fox burial showed. This model produced good agreement indices and passed the X^2 test (df=1 T=3.390(5% 3.841)). We compared dates from the human skeleton and articulated fox skeleton for calculating Differences in OxCal and Intervals in BChron. The modelled Difference was generated by analysing the dates as a Sequence assuming the human skeleton was older than associated materials.

Bradley Fen Hoard 948

We radiocarbon a disarticulated cranial fragment from a Bronze Age hoard (Context 948) at Bradley Fen (Appleby 2005; Gibson & Knight 2006). Two dates had already been obtained from peat within and surrounding the hoard, and the wood of a spear shaft deposited above the hoard (Appleby 2005). Combination of the dates from the peat and the human bone within a phase model including the stratigraphically later date from the spear shaft produces good overall agreement and passes the X^2 test. Unfortunately, the only available account of the radiocarbon dates does not include the laboratory numbers (Gibson & Knight 2006). Difference ranges in OxCal and Intervals in BChron were calculated by comparing the date of the cranial bone against one of the dates from the peat. The modelled Difference was generated by analysing the dates as a Sequence model assuming the disarticulated cranial bone was older than associated materials.

Brigg's Farm (Thorney) 575

We radiocarbon dated a disarticulated human femur and a disarticulated faunal bone from the same context (575) in a settlement ditch (Pickstone & Mortimer 2011). A disarticulated faunal bone from a stratigraphically earlier context had been radiocarbon dated previously. We analysed these three dates in a Sequence model with the disarticulated human and faunal bones from the same context placed in a Combine model (Figures S7–S8). The model produced poor agreement indices and the Combine aspect failed the X^2 test. This was because the human bone was anomalously old – not just older than the faunal bone it was associated with, but also the faunal bone in the earlier stratigraphic unit. We compared the date from the disarticulated human bone against the disarticulated faunal bone from the same context to

generate Differences in OxCal and Intervals in BChron (Figures S9–S10). The modelled Difference was generated by analysing the dates as a Sequence assuming the disarticulated fibula was older than the material in the same and earlier contexts.

```
Plot()
 {
  Sequence("Thorney_575_seq")
  {
   Boundary("Thorney_575_start");
   R_Date("SUERC-25578", 3050, 40);
                                  Combine("575_Combine")
   {
    R_Date("BRAMS-1583", 3334, 27);
    R_Date("BRAMS-1950", 3121, 26);
   };
   Boundary("Thorney_575_send");
  };
 };
```

Figure S7. OxCal script for the Briggs Farm Phase model.

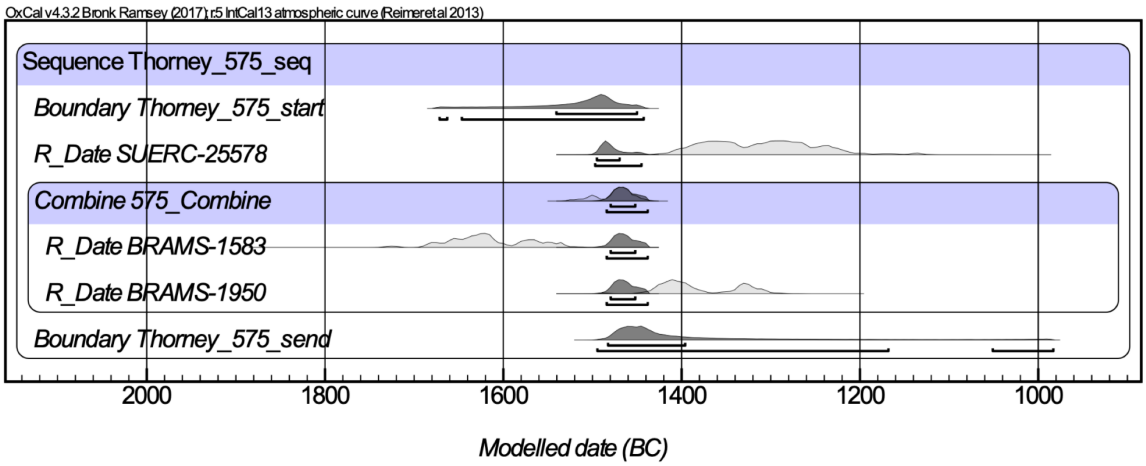

Figure S8. Briggs Farm Phase model.

```
Plot()
 {
  Sequence("Thorney_575_seq")
                                                {
   Boundary("Thorney_575_start");
                                    R_Date("BRAMS-1583", 3334, 27);
   R_Date("SUERC-25578", 3050, 40);
   R_Date("BRAMS-1950", 3121, 26);
   Boundary("Thorney_575_send");
   Difference("Thorney_575_diff", "BRAMS-1583", "BRAMS-1950");
  };
 };
```

Figure S9. OxCal script for the Briggs Farm Curation sequence.

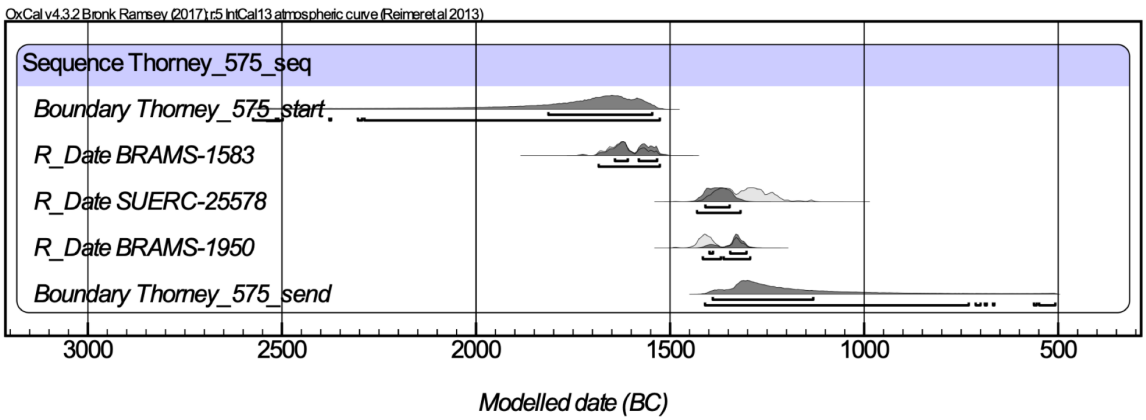

Figure S10. Brigg's Farm Curation sequence.

Canada Farm F.1

We used radiocarbon dates generated by Smith *et al*. (2016) for a complete skeleton F.1, a coffined primary burial from a ring ditch monument. The skeleton was in partial disarticulation, despite the grave showing no signs of disturbance. Histological analysis of this skeleton suggested that the body may have been mummified and potentially curated (Booth *et al*. 2015; Smith *et al*. 2016). Two radiocarbon dates had been generated for this skeleton, producing statistically inconsistent results, although Smith *et al*. (2016) noted that both dates were much earlier than what would be expected from the typology of the accompanying Beaker pot. We used the younger of these dates from the skeleton in our analysis and compared it to a calendrical date range based on the typology of the Beaker pot (2300–2100 BC). Combination of these dates using the Combine function in OxCal assuming the dates related to the same event produces poor agreement indices but passes the X^2 Test (df=1 T=2.225(5% 3.841)). We also compared these two dates to produce Differences in OxCal. The modelled Difference was generated by analysing the dates as a Sequence assuming the human skeleton was older than the accompanying Beaker pot. We generated a radiocarbon determination from the calendrical date range for the typology of the Beaker pot using R_Simulate to compare against the date from F.1 to produce an Interval in BChron.

Cladh Hallan

We ran the chronological model run on previously-obtained radiocarbon dates from Cladh Hallan published in Parker Pearson *et al*. (2005, 2007; Figures S11–S12) and based on the stratigraphic information from the site. This model included dates complete articulated human skeletons (2638 and 2613) buried beneath the floor of the North House, which were

both composed of the partially disarticulated remains of several individuals. Histological analysis of one of the skeletons suggested that parts of it at least had been formerly mummified. Only the tibia from the adult male skeleton (2638) showed poor overall agreement within this model because of it being too old. We compared radiocarbon dates from each skeletal element representing a different individual buried beneath the North House to the modelled OSL dates from the burial sediment to generate modelled Differences in OxCal. We compared radiocarbon dates from the same skeletal elements to a radiocarbon date from a charred barley seed from the house floors covering the burials to generate unmodeled Differences in OxCal and Intervals in BChron (Figures S13–S14). The charred barley seed was stratigraphically later than the human skeletons, however its radiocarbon date was consistent with optically stimulated luminescence (OSL) dates from the graves, as well as some of the radiocarbon dates from some of the buried bones, suggesting any difference between the dates of the burials and constructions of the house floors was within radiocarbon error. We used the radiocarbon dates from the charred seeds over the OSL dates from the burial sediment for producing unmodeled Differences in OxCal and Intervals in OxCal as the OSL date ranges were very wide and produced large Difference/Interval ranges which had limited use. The modelled Difference was generated by analysing the dates as a Sequence assuming the human bones were older than the OSL dates from the sediment and thee radiocarbon dates from the charred seed.

```
Plot("Cladh_Hallan")
 {
  Sequence("Cladh_Hallan_seq")
  {
   Boundary("Cladh_Hallan_start");
   Phase("Cremation_cemetery")
   {
    R_Date("SUERC-10717", 3375, 35);
    R_Date("SUERC-10716", 3270, 35);
   };
   R_Date("SUERC-10818", 3040, 35);
   Phase("Phase_Houses")
   {
    Sequence("Sequence_north")
    {
     Boundary("North_House_start");
     C_Date("CLH03-01", -990, 310);
     Phase("Phase_burials")
     {
      R_Combine("Adult female femur")
      {
       R_Date("GU-9839", 3025, 55);
       R_Date("GU-10489", 2950, 35);
      };
      R_Combine("Adult male skull")
      {
       R_Date("GU-9854", 3105, 50);
       R_Date("GU-10491", 3135, 55);
      };
      R_Combine("Adult Male Tibia")
      {
       R_Date("GU-10488", 3155, 60);
       R_Date("GU-9837", 3305, 55);
      };
      R_Date("GU-9838", 3105, 50);
     };
     Combine("Floor_Construction")
     {
      R_Date("GU-10647", 2915, 40);
      R_Date("SU-10648", 3000, 40);
     };
     Boundary("North_House_end");
    };
    Sequence("Sequence_south")
    {
     C_Date("CLH02-12", -1040, 210);
     Curve("IntCal13","IntCal13.14c");
     Curve("Marine13","Marine13.14c");
     Delta_R("LocalMarine",-68,90);
     Mix_Curve("Mixed","IntCal13","LocalMarine",16,10);
     R_Date("GU-9841", 3070, 50);
    };
    Sequence("Sequence_middle_house")
    {
     C_Date("CLH02-16", -1060, 210);
     Phase("Phase_cist_and_burial")
     {
      R_Date("GU-9844", 2865, 55);
      R_Date("GU-9840", 2845, 50);
     };
    };
   };
   Boundary("Cladh_Hallan_End");
  };
 };
```

Figure S11. OxCal script for the Cladh Hallan phase model.

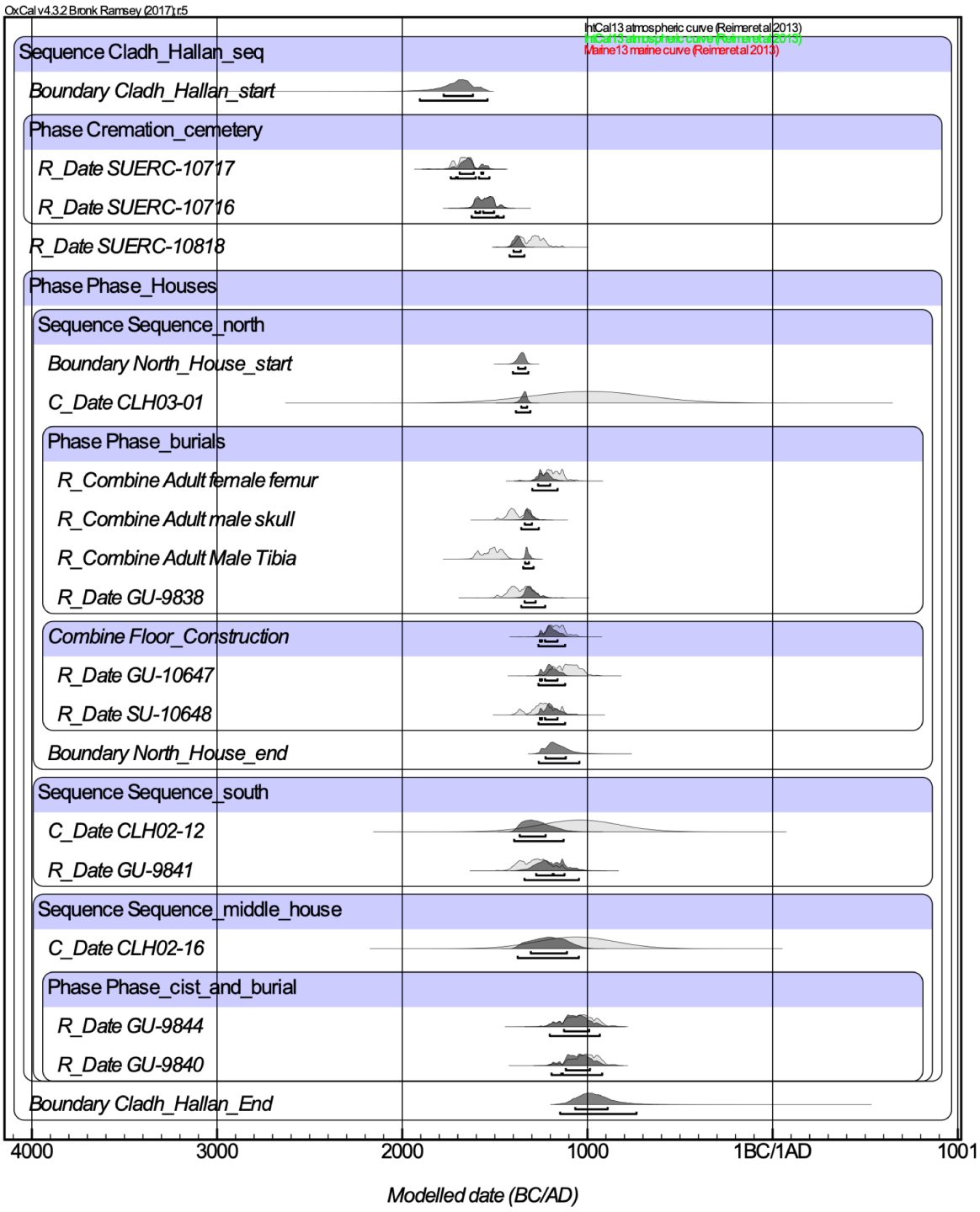

Figure S11. Cladh Hallan phase model.

```
Plot("Cladh_Hallan")
 {
  Sequence("Cladh_Hallan_seq")
  {
   Boundary("Cladh_Hallan_start");
   Phase("Pre_roundhouse_phase")
   {
    Sequence("Cremation_Cemetery_U_House_Sequence")
    {
     Phase("Cremation_cemetery")
     {
      R_Date("SUERC-10717", 3375, 35);
      R_Date("SUERC-10716", 3270, 35);
     };
     R_Date("SUERC-10818", 3040, 35);
    };
    Phase("Burials")
    {
     R_Combine("Adult female femur")
     {
      R_Date("GU-9839", 3025, 55);
      R_Date("GU-10489", 2950, 35);
     };
     R_Combine("Adult male skull")
     {
      R_Date("GU-9854", 3105, 50);
      R_Date("GU-10491", 3135, 55);
     };
     R_Combine("Adult Male Tibia")
     {
      R_Date("GU-10488", 3155, 60);
      R_Date("GU-9837", 3305, 55);
     };
     R_Date("GU-9838", 3105, 50);
    };
   };
   Phase("Phase_Houses")
   {
    Sequence("Sequence_north")
    {
     Boundary("North_House_Start");
     C_Date("CLH03-01", -990, 310);
     Combine("Floor_Construction")
     {
      R_Date("GU-10647", 2915, 40);
      R_Date("SU-10648", 3000, 40);
     };
     Boundary("North_House_End");
    };
    Sequence("Sequence_south")
    {
     C_Date("CLH02-12", -1040, 210);
     Curve("IntCal13","IntCal13.14c");
     Curve("Marine13","Marine13.14c");
     Delta_R("LocalMarine",-68,90);
     Mix_Curve("Mixed","IntCal13","LocalMarine",16,10);
     R_Date("GU-9841", 3070, 50);
    };
    Sequence("Sequence_middle_house")
    {
     C_Date("CLH02-16", -1060, 210);
     Phase("Phase_cist_and_burial")
     {
      R_Date("GU-9844", 2865, 55);
      R_Date("GU-9840", 2845, 50);
     };
    };
   };
   Boundary("Cladh_Hallan_End");
   Difference("2613_diff", "Adult female femur", "CLH03-01");
   Difference("2638_skull_diff", "Adult male skull", "CLH03-01");
   Difference("2638_tibia_diff", "Adult Male Tibia", "CLH03-01");
   Difference("2638_mandible_diff", "GU-9838", "CLH03-01");
   Difference("2638_mandible_diff4", "GU-9838", "SU-10648");
   Difference("2638_tibia_diff4", "Adult Male Tibia", "SU-10648");
   Difference("2638_skull_diff4", "Adult male skull", "SU-10648");
   Difference("2613_diff4", "Adult female femur", "SU-10648");
  };
 };
```

Figure S12. OxCal script for the Cladh Hallan Curation sequence.

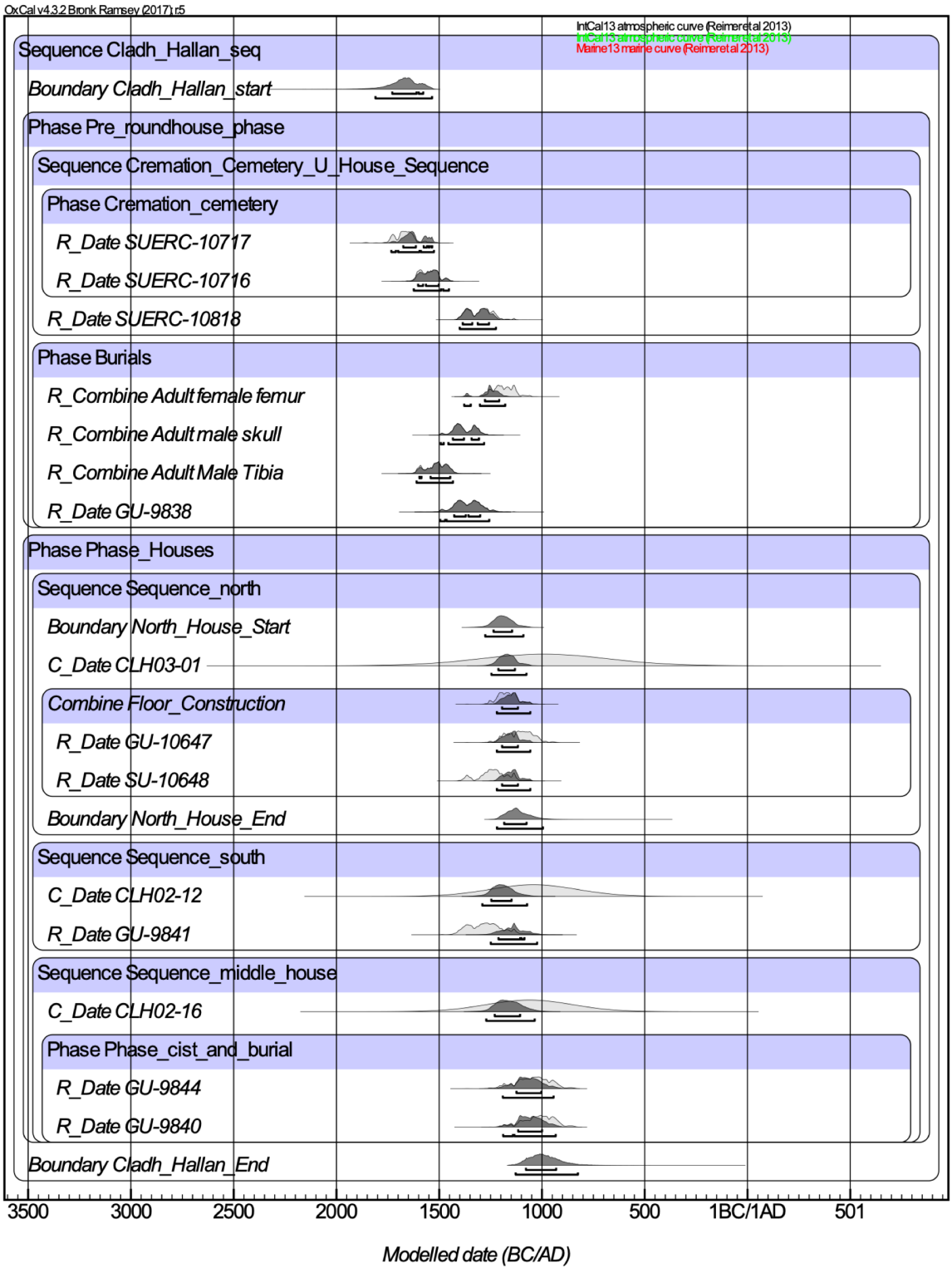

Figure S13. Cladh Hallan Curation sequence.

Clay Farm 2910 (Context 925)

We radiocarbon dated a disarticulated human cranial fragment that had been deposited in a settlement enclosure ditch terminal (2910; Mortimer & Phillips 2012). We placed the date in

a Sequence model with radiocarbon dates from already obtained from a disarticulated animal bone and charred seeds from earlier stratigraphic units. The Sequence model produced good agreement indices (Figure S15–S16). We generated Differences in OxCal and Intervals in BChron by comparing the date from the disarticulated human cranial bone against the date from the disarticulated faunal bone from and early context as a *terminus ante quem* (Figure S17–S18). The modelled Difference was generated by analysing the dates as a Sequence assuming the disarticulated human cranial fragment was older than materials from earlier stratigraphic units.

```
Plot()
 {
  Sequence("925")
  {
   Boundary("Start");
   R_Date("SUERC-35980", 3065, 30);
   R_Date("SUERC-35979", 3080, 30);
   R_Date("BRAMS-1308", 3077, 25);
   Boundary("End");
  };
 };
```

Figure S14. OxCal script for the Clay Farm 2910 phase model.

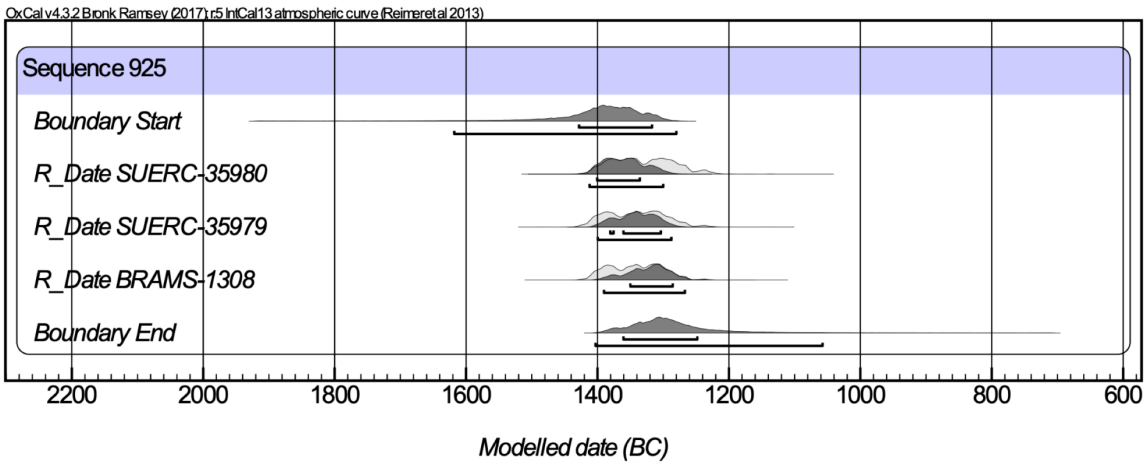

Figure S15. Clay Farm 2910 phase model.

```
Plot()
 {
  Sequence("925")
  {
   Boundary("Start");
   R_Date("BRAMS-1308", 3077, 25);
   R_Date("SUERC-35980", 3065, 30);
   R_Date("SUERC-35979", 3080, 30);
   Difference("D_Clay_Farm_2910", "BRAMS-1308", "SUERC-35980");
   Boundary("End");
  };
 };
```

Figure S16. OxCal script for the Clay Farm 2910 Curation sequence.

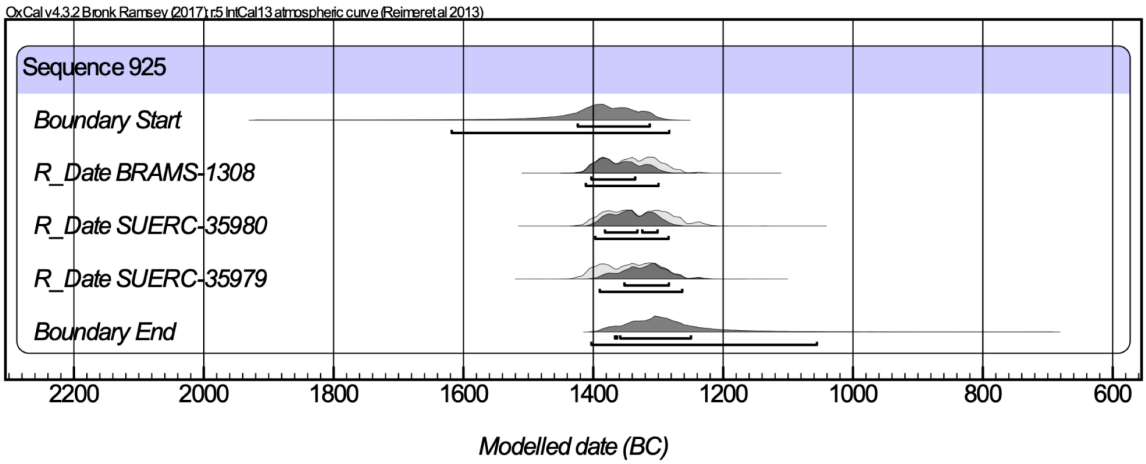

Figure S17. Clay Farm 2910 Curation sequence.

Clay Farm 6319

We radiocarbon dated a disarticulated human cranial fragment from a settlement pit (6319) to compare to a radiocarbon date from a disarticulated faunal bone from an underlying context in the same pit (Mortimer & Phillips 2012). We put the dates in a Sequence model reflecting their stratigraphic relationship. The model shows poor agreement indices, with the human cranial bone coming out as older than the disarticulated faunal bone, despite the animal bone coming from an earlier context (Figures S19–S20). We compared the two dates directly to calculate Differences in OxCal. We produced modelled Sequences by comparing dates in a Sequence model assuming the disarticulated cranial fragment was older than the disarticulated faunal bone from the underlying context. We did not calculate an Interval in BChron for this deposit for the analysis of combined Intervals, as it dates to the Iron Age (Figures S21–S22).

```
Plot()
 {
  Sequence("Clay_Farm_6319")
  {
   Boundary("start");
   R_Date("SUERC-35986", 2410, 30);
   R_Date("SUERC-38465", 2550, 30);
   Boundary("end");
  };
 };
```

Figure S18. OxCal script for the Clay Farm 6319 sequence.

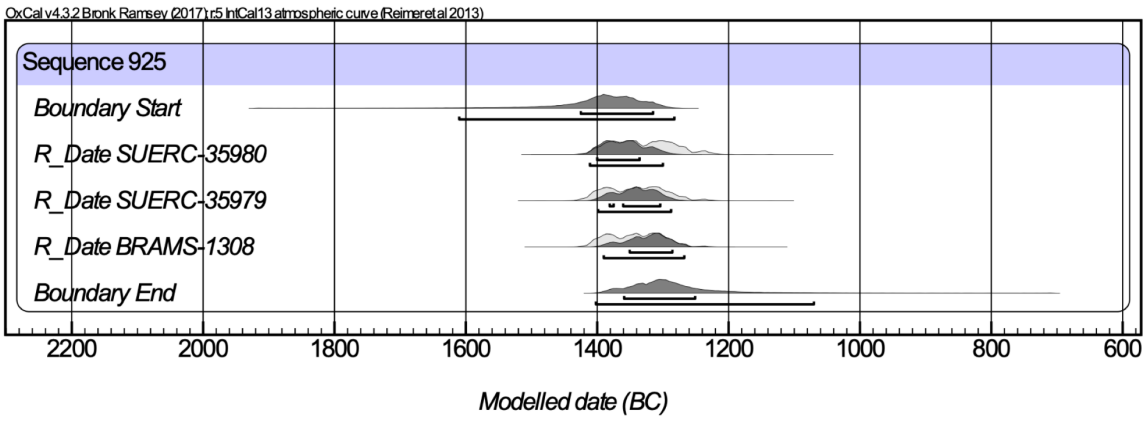

Figure S19. Clay Farm 6319 sequence.

```
Plot()
 {
  Sequence("Clay_Farm_6319")
  {
   Boundary("start");
   R_Date("SUERC-38465", 2550, 30);
   R_Date("SUERC-35986", 2410, 30);
   Boundary("end");
  };
  Difference("D_Clay_Farm_6319", "SUERC-38465", "SUERC-35986");
 };
```

Figure S20. OxCal script for the Clay Farm 6319 Curation sequence.

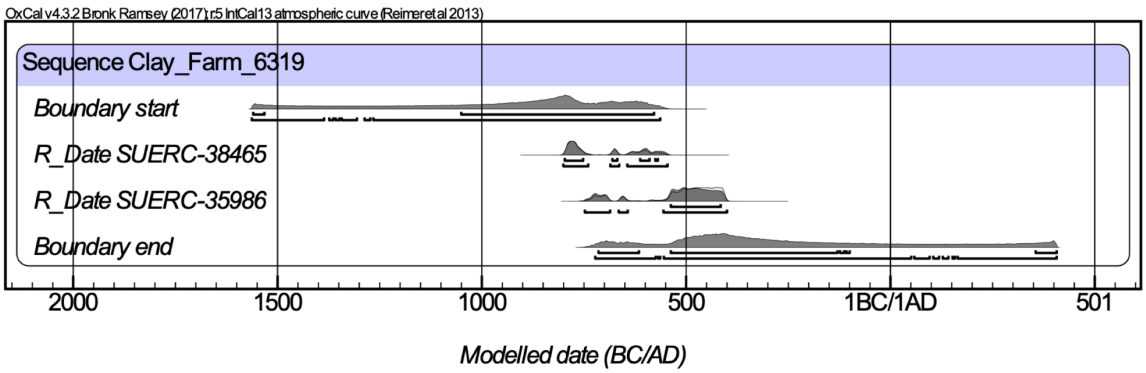

Figure S21. Clay Farm 6319 Curation sequence.

Cliff's End Farm

We did not obtain any new radiocarbon dates for Cliff's End Farm, but reran radiocarbon dates that had already been obtained and used in the chronological phase model of McKinley *et al*. (2014), which was based on the site stratigraphy. We were focussing on a series of deposits of disarticulated and partially articulated human remains as showing potential for having been curated. We changed the model slightly to include the disarticulated bones in a Phase together to test whether any of the radiocarbon dates were anomalously old, and at the same time produce modelled Differences assuming the disarticulated bones were older than material from the same phase (Figures S23–24). Only one of the deposits of disarticulated human bones we included produced a date that produced poor agreement indices and was anomalously old (ON110). We compared each date against the boundary for the beginning of the 3666 phase, the context from which the disarticulated bone was recovered, to produce modelled Differences in OxCal. To produce an unmodeled Difference carrying no assumptions, we tested each date from the disarticulated bones against a simulated (using the R_Simulate function in OxCal) radiocarbon determination representing the 95% confidence range of the context 3666 start boundary. We compared the same dates for calculating unmodeled Intervals in BChron.

```
Plot()
 {
  Phase("Phase 2018")
  {
   Sequence("3666")
   {
    Boundary("start_3666");
    Phase("3666")
    {
     After("pit 3666 satellites disarticulated")
     {
      R_Combine("184605")
      {
       R_Date("OxA-18433", 2748, 27);
       R_Date("OxA-18434", 2693, 27);
      };
      R_Combine("124205")
      {
       R_Date("OxA-18437", 2703, 28);
       R_Date("GrA-37709", 2700, 30);
      };
      R_Date("OxA-18439", 2692, 28);
      R_Date("GrA-37912", 2740, 30);
      R_Date("GrA-37913", 2740, 30);
      R_Date("GrA-37713", 2735, 30);
     };
     Sequence("Pit 3666")
     {
      Phase("Disarticulated bones")
      {
       R_Date("KIA-24861", 2865, 29);
       R_Date("GrA-37966", 2710, 30);
       R_Date("GrA-37751", 2790, 30);
       R_Date("OxA-18435", 2728, 28);
       R_Date("OxA-18436", 2748, 29);
      };
      Boundary("3666_1_Start");
      Phase("3666_1")
      {
       Sequence("burial 3873")
       {
        R_Date("GrA-35999", 2730, 35);
        R_Date("OxA-17804", 2713, 29);
       };
       Sequence("Pit 3666_2")
       {
        R_Combine("bone_gp_637")
        {
         R_Date("OxA-17807", 2760, 35);
         R_Date("GrA-36003", 2710, 35);
        };
        Phase("Above ABG 637")
        {
         Sequence("Unnamed")
         {
          R_Date("OxA-17805", 2677, 30);
          Phase("[3674] & [3680]")
          {
           R_Date("OxA-18597  [3674]", 2754, 27);
           R_Date("OxA-18431", 2767, 29);
           Phase("[3680]")
           {
            R_Combine("cattle skull")
            {
             R_Date("OxA-17806", 2766, 28);
             R_Date("GrA-36003", 2710, 35);
            };
            R_Date("GrA-36002", 2750, 35);
           };
          };
         };
         R_Date("GrA-36000", 2745, 35);
        };
       };
      };
      Boundary("3666_1_End");
      R_Date("OxA-18429", 2698, 27);
     };
    };
    Boundary("end_3666");
    R_Date("Sim_3666_start", 2717, 24);
    Difference("ON 101_diff", "GrA-37751", "3666_1_Start");
    Difference("ON 100_diff", "GrA-37966", "3666_1_Start");
    Difference("ON 536_diff", "OxA-18435", "3666_1_Start");
    Difference("ON 106_diff", "OxA-18436", "3666_1_Start");
    Difference("ON 110_diff", "KIA-24861", "3666_1_Start");
    Difference("ON 101_diff", "GrA-37751", "Sim_3666_start");
    Difference("ON 100_diff", "GrA-37966", "Sim_3666_start");
    Difference("ON 536_diff", "OxA-18435", "Sim_3666_start");
    Difference("ON 106_diff", "OxA-18436", "Sim_3666_start");
    Difference("ON 110_diff", "KIA-24861", "Sim_3666_start");
   };
  };
 };
```

Figure S22. OxCal script for the Cliff's End Farm phase model.

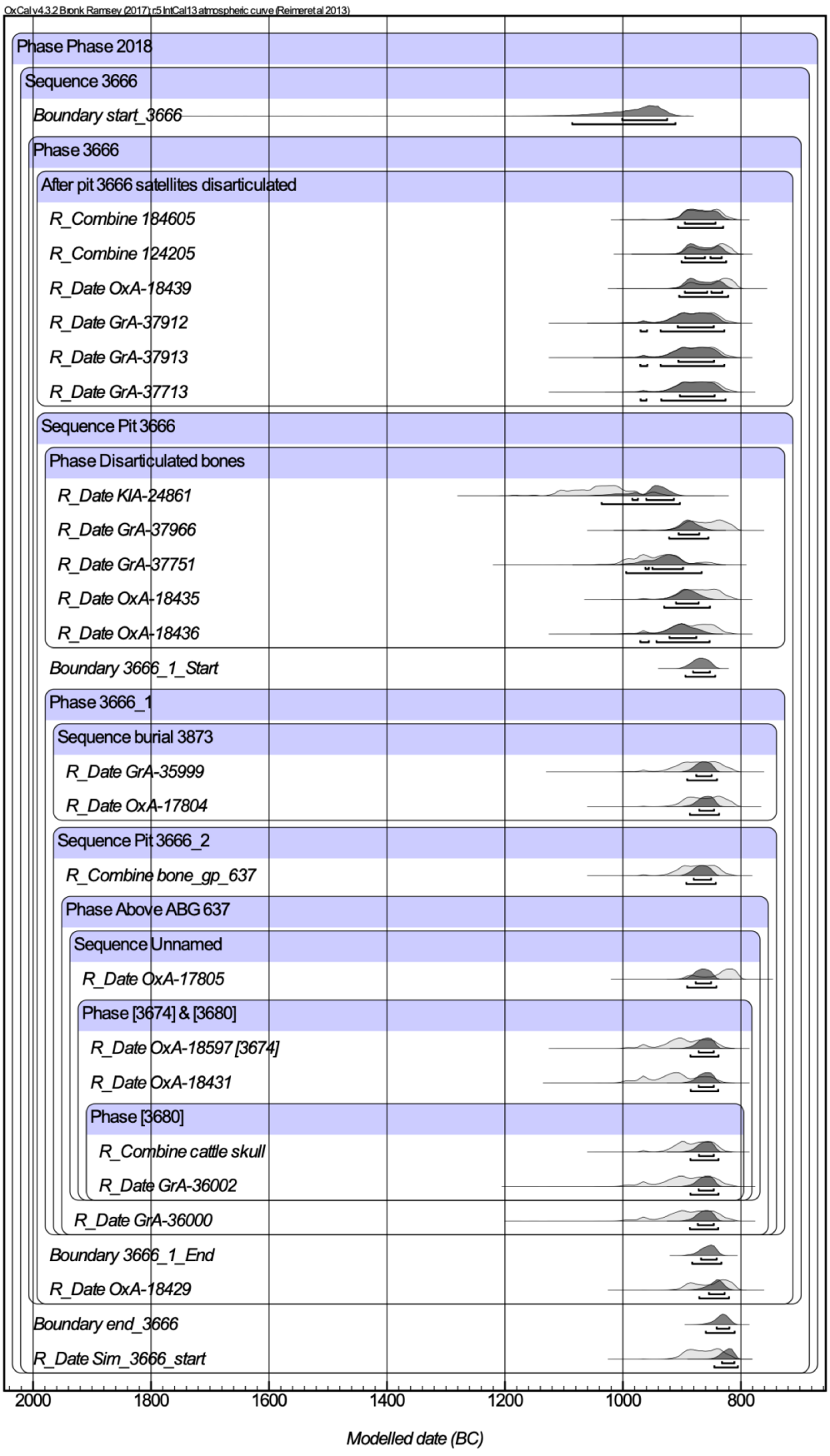

Figure S23. Cliff's End Farm Curation sequence.

Cnip Headland Area A

We used previously published radiocarbon dates from Area A of Cnip Headland comprising disarticulated and partially articulated human bones recovered from a stone cist (Lelong *et al*. 2016). We compared all dates of disarticulated bones against a disarticulated human metacarpal from the basal deposit in the cist. Most of the disarticulated human bones came from a later stratigraphic unit than the human metacarpal. These dates were put into a Sequence model based on their stratigraphic relationships. The dates from the human metacarpal in the basal fill showed poor overall agreement in the model (Figures S25–S26). This was because the other disarticulated human bones were older than the human metacarpal, despite them having been retrieved from stratigraphically contemporary or later deposits. This anomalous result could be due to an errant radiocarbon date having been generated from the human metacarpal in the basal fill, however, it is equally possible that the disarticulated bones from the later deposit were already old when they were interred in the cist. Dates from each disarticulated bone were compared against the date of the metacarpal from the basal fill for the calculation of Differences in OxCal and Intervals in BChron (Figures S27–S28). We produced modelled Differences by comparing dates in a Sequence model assuming that the disarticulated bones were older than the human metacarpal from thee basal fill.

```
Plot()
 {
  Sequence("Cnip Area A")
  {
   Boundary("Start");
   Phase("014")
   {
    R_Date("SUERC-30860", 3335, 35);
    R_Date("SUERC-30859", 3430, 35);
   };
   Phase("005")
   {
    R_Combine("Sk 1")
    {
     R_Date("SUERC-30853", 3435, 35);
     R_Date("SUERC-39858", 3430, 35);
    };
    R_Date("SUERC-39854", 3410, 35);
   };
   Boundary("End");
  };
 };
```

Figure S24. OxCal script for the Cnip Headland Area A phase model.

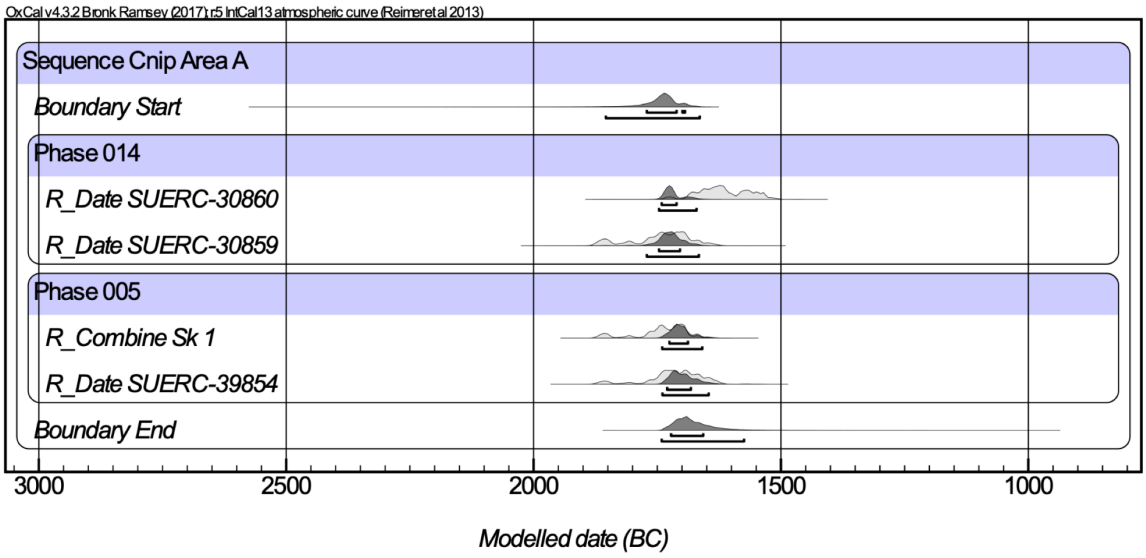

Figure S25. Cnip Headland Area A phase model.

```
Plot()
 {
  Sequence("Cnip Area A")
  {
   Boundary("Start");
   Phase("Curated_Bone")
   {
    R_Date("SUERC-30859", 3430, 35);
    R_Combine("Sk 1")
    {
     R_Date("SUERC-30853", 3435, 35);
     R_Date("SUERC-39858", 3430, 35);
    };
    R_Date("SUERC-39854", 3410, 35);
   };
   R_Date("SUERC-30860", 3335, 35);
   Boundary("End");
   Difference("Cnip_Sk_1_diff", "Sk 1", "SUERC-30860");
   Difference("Cnip_SF62_diff", "SUERC-39854", "SUERC-30860");
   Difference("Cnip_SF54b_diff", "SUERC-30859", "SUERC-30860");
  };
 };
```

Figure S26. OxCal scipt for the Cnip Headland Area A Curation sequence.

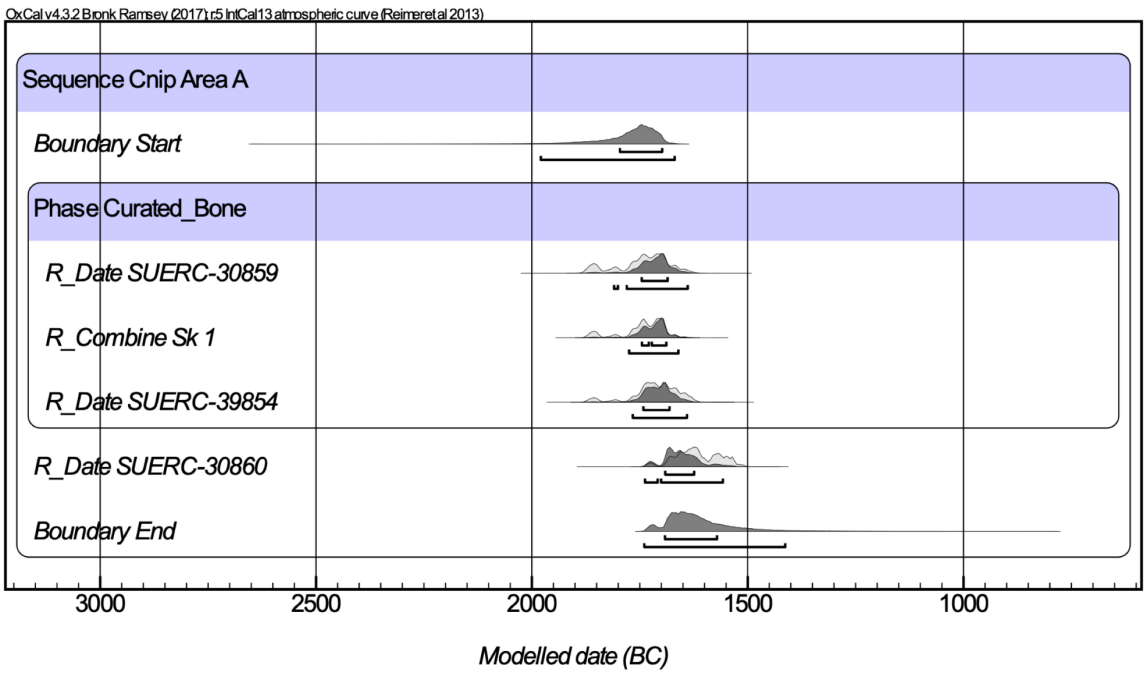

Figure S27. Cnip Headland Area A Curation sequence.

Cotswold Community

Context 7971 at Cotswold Community was a context within a pit which contained a pair of disarticulated human femoral fragments (presumably from the same individual) with some burnt bone, a charred hazelnut seed, charcoal and some fragmentary Beaker pottery (Smith *et al*. 2010). We obtained dates from one of the disarticulated human femora, the charred hazelnut, some charcoal and a fragment burnt bone. Attempts to combine the dates from these materials using the Combine function in OxCal failed the X^2 test 2-Test: (df=3 T=43.074(5% 7.8)). However, this failure was mainly due to the date from the charred hazelnut seed, which was significantly older than the dates from the other materials. However, when the charred hazelnut seed was removed from the Combine model, the model still shows poor agreement indices and failed the X^2 test because the human bone was anomalously old (df=2 T=9.845(5% 6.0)). The dates from the burnt bone and ash charcoal are consistent with one another. We compared the date from the human bone against the date from the burnt bone to calculate Differences in OxCal and Intervals in BChron. Modelled Differences were produce by placing the dates in a Sequence model assuming the human bone femur was older than the associated materials.

Dryburn Bridge Cist 1

Dryburn Bridge Cist 1 consisted of a stone cist containing a complete articulated skeleton (Burial 5) covered by the disarticulated incomplete remains of a second individual (Burial 4). We combined previously-published dates on human remains (Dunwell *et al*. 2007). Combination of these dates using the Combine function produced good agreement indices and passed the X^2 test (df=1, T=0.460(5% 3.841)). We compared these two dates for calculating Differences in OxCal and Intervals in BChron. Modelled Differences were calculated in OxCal by placing dates in Sequence model which assumed that Burial 4 was older than Burial 5.

Dryburn Bridge Cist 2

The human remains from Dryburn Bridge Cist 2 consisted of a complete articulated human skeleton (Burial 10) covered by the incomplete disarticulated remains of a second individual (Burial 11). We used radiocarbon dates that had been published previously in Dunwell *et al*. (2007). Combination of these dates using the Combine function produced good agreement indices and passed the X^2 Test (df=1, T=0.182(5% 3.841)). We calculated Differences in OxCal and Intervals in BChron by comparing the date from Burial 11 against the date from Burial 10. We produced modelled Differences by comparing dates in a Sequence model where Burial 11 was assumed to be older than Burial 10.

East Chisenbury 128

The East Chisenbury 128 bones were recovered from a discrete context (128) in a ditch surrounding a settlement (Phil Andrews, Wessex Archaeology, *pers. comm.*). We radiocarbon dated a disarticulated human ulna showing cortical weathering and a disarticulated faunal bone from the same context. Attempts to combine the dates from these two bones using the Combine function in OxCal produced poor agreement indices and failed the X^2 test, as the disarticulated human bone was anomalously older than the accompanying faunal bone (df=1 T=31.257(5% 3.8)). We compared these two dates to produce Differences in OxCal and Intervals in BChron. We produced modelled Differences by comparing dates in a Sequence model where the human bone was assumed to be older than the associated faunal remains.

East Chisenbury 140

The East Chisenbury 140 bones were recovered from a context in a post hole on a settlement (Phil Andrews, Wessex Archaeology, personal communication). We radiocarbon dated a disarticulated human left radius and a disarticulated animal bone from the same context

(140). Combining these dates using the Combine function in OxCal, assuming that they represent the same event produces poor agreement indices and fails the X^2 test (df=1 T=41.517(5% 3.8)). However, this poor agreement was due to an anomalously early date from the faunal bone, not the human remains. Either the date from the animal bone is erroneous, or the disarticulated faunal bone was already old when it was deposited. We compared these two dates in our calculations of Differences in OxCal and Intervals in BChron. We produced modelled Differences by comparing dates in a Sequence model where the human bone was assumed to be older than the associated faunal bone.

East Chisenbury 152

The East Chisenbury 152 were retrieved from a context (152) in a pit on a settlement (Phil Andrews, Wessex Archaeology, personal communication). We radiocarbon dated a disarticulated human cranial fragment showing perimortem trauma and a disarticulated faunal bone from the same context. Combination of these two dates using the Combine function in OxCal assuming that they date the same event produced good agreement indices and passed the X^2 test (df=1, T=1.986(5% 3.841)). We compared these two dates to produce Differences in OxCal and Intervals in BChron. We produced modelled Differences by comparing dates in a Sequence model where the human bone was assumed to be older than the associated faunal bone.

East Chisenbury 201

We radiocarbon dated a disarticulated human cranial fragment and a disarticulated animal bone from context 201 in an occupation deposit on a settlement (Phil Andrews, Wessex Archaeology, *pers. comm.*). Combination of the two dates using the Combine function in OxCal, assuming the dates refer to the same event, produced good agreement indices and passed the X^2 test (df=1 T=0.003(5% 3.841)). These two dates were compared to produce Differences in OxCal and Intervals in BChron. We produced modelled Differences by comparing dates in a Sequence model where the human bone was assumed to be older than the associated faunal bone.

East Chisenbury 600

We radiocarbon dated a disarticulated right human frontal and a disarticulated faunal bone from context 600, a deposit of occupation debris, or possible badger spoil on a settlement (Phil Andrews, Wessex Archaeology, *pers. comm.*). Combination of the two dates using the

Combine function un OxCal assuming the dates were related to the same event produced poor agreement indices and failed the X^2 test, as the date from the human bone was anomalously old (df=1 T=49.509(5% 3.8)). We compared these two dates to produce Differences in OxCal and Intervals in BChron. We produced modelled Differences by comparing dates in a Sequence model where the human bone was assumed to be older than the associated faunal bone.

Eye Quarry 2222

We radiocarbon dated a disarticulated human frontal bone and a disarticulated faunal bone from Eye Quarry Context 2222, a deposit in a settlement pit (Patten 2004). Combination of these dates using the Combine function in OxCal produced good agreement indices and passed the X^2 test (df=1 T=0.615(5% 3.841)). These dates were compared to produce Differences in OxCal and Intervals in OxCal. We produced modelled Differences by comparing dates in a Sequence model assuming the human frontal bone was older than the associated disarticulated faunal bone.

Eye Quarry F.2623

We radiocarbon dated a disarticulated human mandible and a disarticulated faunal bone from the same context (F.2623) in a pit on a settlement (Patten 2004). Combination of the two dates using the Combine function in OxCal produced good agreement indices and passed the X^2 test (df=1 T=0.329(5% 3.841). We compared these two dates to produce Differences in OxCal and Intervals in BChron. We produced modelled Differences by comparing dates in a Sequence model assuming that the disarticulated human mandible was older than the disarticulated faunal bone.

Greylake

We radiocarbon dated a disarticulated human left humerus and two sheep mandibles from a deposit associated with a wooden platform that had been dated by dendrochronology to 958 BC (Brunning 1997). We modelled the dates as a Sequence, which included a calendrical date (C_date in OxCal) for the wooden structure. The model showed good overall agreement, although the date from one of the sheep mandibles showed poor individual agreement indices because it was anomalously old. It is possible that this sheep mandible produced on erroneous date or that the mandible itself had been curated. We compared the radiocarbon date from the human humerus against the calendrical date for the wooden structure to produce Differences

in OxCal. We produced a modelled Difference by comparing dates as part of a Sequence assuming the human bone was older than the wooden platform. We compared the date from the disarticulated human humerus against the date from the younger sheep mandible for the calculation of an Interval in BChron.

Ingleby Barwick (Windmill Fields)

Windmill Fields comprises a small Bronze Age cemetery including furnished complete articulated burials, unfurnished burials and a wooden cist containing the partial disarticulated remains of multiple individuals (Annis *et al*. 1997). Sk 6 was a complete articulated skeleton from a furnished burial which was accompanied by the disarticulated incomplete remains (mainly crania and long bones) of an additional three individuals (Sk 8). The articulated burial had been radiocarbon dated previously by Tees Archaeology. We obtained radiocarbon dates from two of the disarticulated crania (Sk. 8) which accompanied Sk. 6. We placed the dates from the burials in a Phase model assuming they related to the same broad period of activity. We combined dates from Sk 6 and Sk 8 using the Combine function in OxCal assuming their dates related to the same event. This passed the X^2 test but produced poor agreement indices because the two crania were anomalously old (Figure S29–S30). We produced Differences in OxCal and Intervals in OxCal by comparing each date from the crania against the date from Sk 6 (Figures S31–S32).

```
Plot()
 {
  Sequence("Ingleby Burials")
  {
   Boundary("Burials start");
   Phase("Burials")
   {
    R_Date("UB-4173", 3364, 22);
    Combine("Burial 6")
    {
     R_Date("BRAMS-1286", 3691, 28);
     R_Date("BRAMS-1287", 3691, 28);
     R_Date("UB-4174", 3609, 24);
    };
    R_Date("OxA-8728", 3725, 40);
    R_Date("OxA-8652", 3725, 40);
    R_Date("OxA-8650", 3755, 40);
    R_Date("OxA-8651", 3705, 35);
    R_Date("OxA-8729", 3780, 40);
   };
   Boundary("Burials end");
  };
 };
```

Figure S28. OxCal script for Ingleby Barwick Sk 6 Combine model.

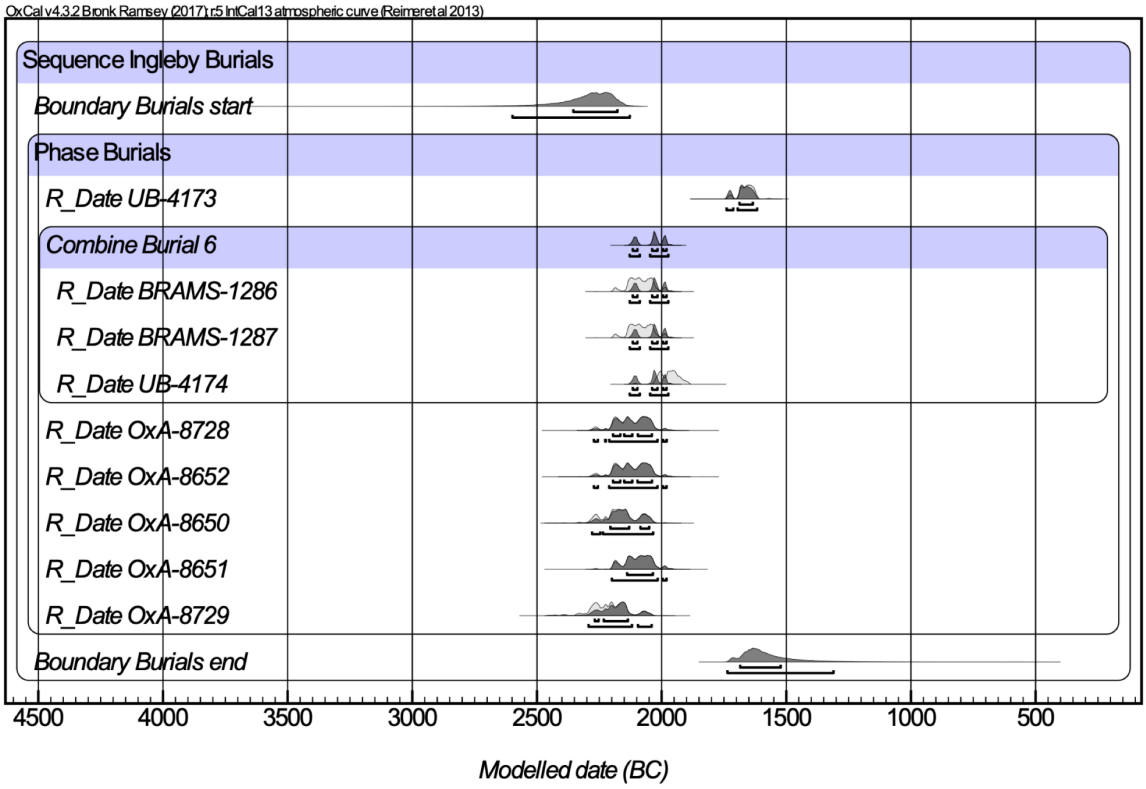

Figure S29. Ingleby Barwick Sk 6 Combine model.

```
Plot()
 {
  Sequence("Ingleby Burials")
  {
   Boundary("Burials start");
   Phase("Burials")
   {
    Sequence("Burial 6")
    {
     Phase("Disarticulated bone")
     {
      R_Date("BRAMS-1286", 3691, 28);
      R_Date("BRAMS-1287", 3691, 28);
     };
     R_Date("UB-4174", 3609, 24);
    };
    Phase("Other Burials")
    {
     R_Date("OxA-8728", 3725, 40);
     R_Date("UB-4173", 3364, 22);
     R_Date("OxA-8652", 3725, 40);
     R_Date("OxA-8650", 3755, 40);
     R_Date("OxA-8729", 3780, 40);
     R_Date("OxA-8651", 3705, 35);
    };
   };
   Boundary("Burials end");
   Difference("D_Ingleby_Barwick_Sk_6", "BRAMS-1286", "UB-4174");
   Difference("Ingleby_Barwick_SK_6b", "BRAMS-1287", "UB-4147");
  };
 };
```

Figure S30. OxCal scipt for Ingleby Barwick Sk 6 Curation sequence.

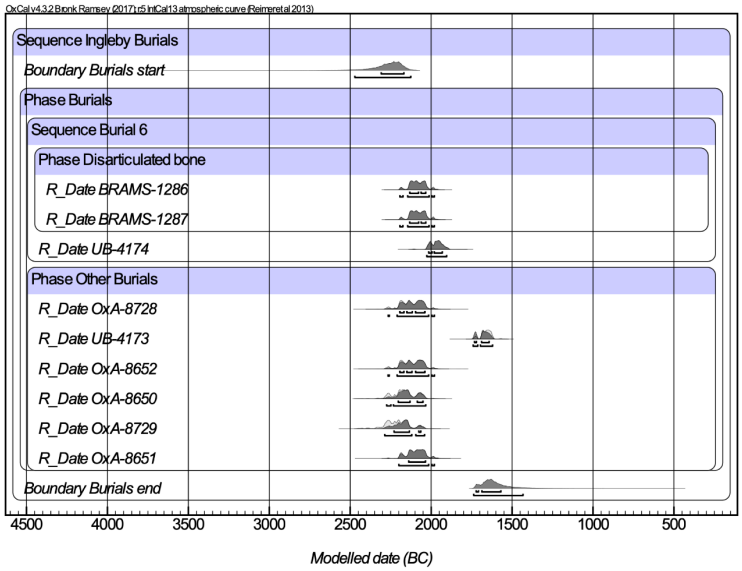

Figure S31. Ingleby Barwick Sk. 6 Curation sequence.

Irthlingborough 6400

Irthlingborough 6400 comprises a cremation representing a minimum of two individuals that had been deposited in a round barrow mound (Harding & Healy 2011). The context had not been truncated, but the cremation deposit was not heavy enough to account for two individuals, suggesting only a portion of one or both individuals had been buried. A radiocarbon date had been obtained previously from the pyre charcoal. We radiocarbon dated two cremated human bones representing discrete individuals. Combination of all three dates using the Combine function in OxCal assuming that all dates referred to the same event produced good agreement indices and passed the X^2 test (df=2 T=2.265(5% 5.991)). We produced Differences in OxCal by comparing the radiocarbon date from the older cremated human bone against a Combine model including the radiocarbon dates from the younger cremated human bone and the pyre material. We produced modelled Differences by comparing the dates in a Sequence assuming one of the cremations was older than the other. We produced Intervals in BChron by comparing the dates from the two cremated human bones.

Irthlingborough 6461

Irthlingborough 6461 consists of a cremation burial representing the remains of at least three individuals deposited in a round barrow mound (Harding & Healy 2011). The weight of the cremation was too low to represent the complete remains of all three individuals, suggesting that one of the individuals at least was only partial. We radiocarbon dated two replicate cremated human bones from this deposit. Combination of these two dates using the Combine function in OxCal assuming they relate to the same event produced good agreement indices and passed the X^2 test (df=1 T=1.435(5% 3.841). We calculated Differences in OxCal and an Interval in BChron by comparing these two dates. Modelled Differences were produced by comparing dates in a Sequence model assuming one of the cremations was older than the other.

Latton Lands 1751

We radiocarbon dated a disarticulated human femur and a disarticulated faunal bone that had been deposited in the same context (1751) in a watering hole (Powell *et al*. 2008). Combination of the dates using the Combine function in OxCal assuming the dates represent the same event produced good agreement indices. We compared these dates to produce Differences in OxCal and Intervals in BChron. We generated modelled Differences by

comparing dates in a Sequence model assuming the disarticulated human femur was older than the associated faunal bone.

Melton Quarry

We analysed unpublished radiocarbon dates obtained from human remains excavated by Oxford Archaeology from Melton Quarry (Fraser Brown and Lauren McIntyre, Oxford Archaeology South, *pers. comm.*). The grave included a complete articulated human skeleton accompanied by the partial disarticulated remains of an infant. Combining the radiocarbon using the Combine function in OxCal assuming the dates related to the same event produced poor agreement indices and failed the X^2 test (df=1 T=27.720(5% 3.8)). We compared these two dates to produce Differences in OxCal and Intervals in BChron. Modelled Differences were produced by comparing the dates in a Sequence which assumed that the partial infant remains were older than the articulated human skeleton.

Needingworth Quarry 3284

We radiocarbon dated a disarticulated femoral fragment showing cortical modifications indicative of carnivore gnawing and a disarticulated complete skeleton from the same buried soil context (3284) on a settlement (Evans & Vander Linden 2009). Combination of the two dates using the Combine function in Oxcal assuming that the dates reflected the same event produced good agreement indices and passed the X^2 test (df=1 T=0.645(5% 3.841)). We compared these two dates to produce Differences in Oxcal and Intervals in BChron. We produced modelled Differences by comparing the dates in a Sequence model assuming that the femoral fragment was older than the disarticulated complete skeleton from the same context.

Needingworth 427

We radiocarbon dated a bone from a set of articulated foot bones to compare to a radiocarbon date that had already been obtained from a disarticulated faunal bone from context 427, located in a natural hollow outside a settlement (Evans & Vander Linden 2009). Combination of the two dates using the Combine function in OxCal produced good agreement indices and passed the X^2 test (df=1 T=2.682(5% 3.841)). We produced Differences in OxCal using these two dates, but did not generate an Interval in BChron, as these remains all dated to the Iron Age. Modelled Differences were generated by comparing the dates in a Sequence model assuming the foot bones were older than the associated faunal bone.

Potterne

We radiocarbon dated a disarticulated human cranial fragment (1016) from Phase 11, two disarticulated human frontal fragments from Phase 10 (2747 and 2776) and a disarticulated right mandible fragment (2033) from Phase 4 in the Potterne midden (Lawson *et al*. 2000). We added these dates to a pre-existing chronological model based on stratigraphic relationships between deposits that had been built from previous radiocarbon dates on charcoal and disarticulated animal bones retrieved from different phases of the midden. The model produced poor agreement indices, mainly because the radiocarbon date of the mandible fragment 2033 was anomalously older than material recovered from the same phase (Figures S33–S34). The rest of the samples produced good agreement indices. We produced Differences in OxCal and Intervals in BChron by comparing dates from the disarticulated human remains against materials recovered from the same contexts (Figures S35–S36).

```
Plot()
 {
  Sequence("Potterne_seq")
  {
   Boundary("Potterne_start");
   Phase("Phase_11")
   {
    R_Date("HAR-6983", 3430, 100);
    R_Date("HAR-6982", 3130, 100);
    R_Date("BRAMS-1590", 2768, 27);
   };
   Phase("Phase 10")
   {
    R_Date("BRAMS-1587", 2689, 27);
    R_Date("BRAMS-1582", 2701, 26);
   };
   Sequence("Sequence_2")
   {
    After("TPQ5")
    {
     R_Date("HAR-8938", 3000, 90);
    };
    Combine("Phase_7_comb")
    {
     R_Date("HAR-6980", 2650, 80);
     R_Date("HAR-6981", 2630, 70);
    };
   };
   R_Date("BRAMS-1298", 2828, 27);
   Phase("Phase_4")
   {
    R_Date("HAR-6979", 2490, 70);
    R_Date("HAR-6978", 2590, 80);
   };
   Boundary("Potterne_end");
  };
 };
```

Figure S32. OxCal script for the Potterne phase model.

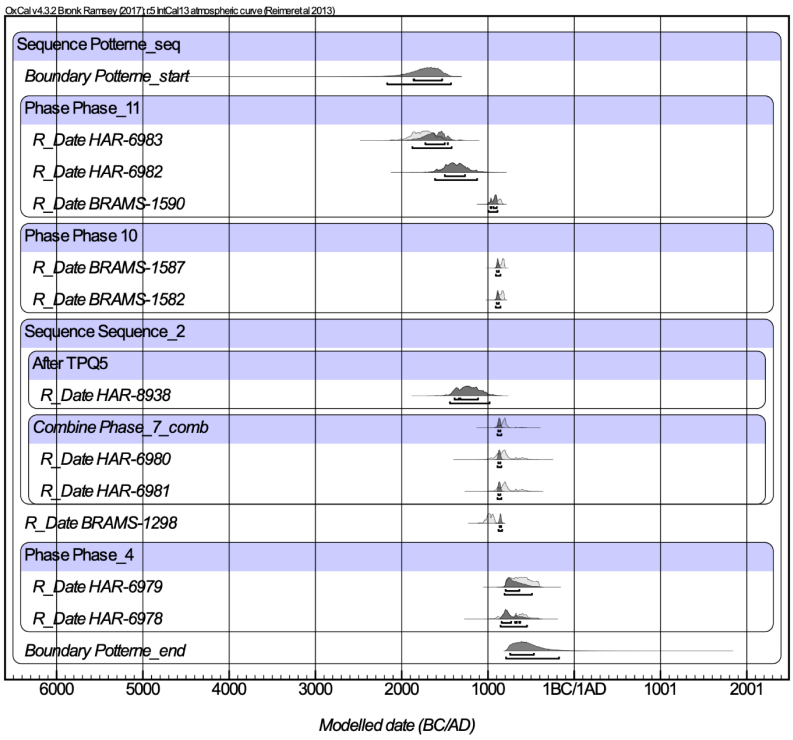

Figure S33. Potterne phase model.

```
Plot()
 {
  Phase("Disarticulated Bone2")
  {
   R_Date("BRAMS-1590", 2768, 27);
   R_Date("BRAMS-1298", 2828, 27);
   R_Date("BRAMS-1587", 2689, 27);
   R_Date("BRAMS-1582", 2701, 26);
   Sequence("Potterne_seq")
   {
    Boundary("Potterne_start");
    Phase("Phase_11")
    {
     R_Date("HAR-6983", 3430, 100);
     R_Date("HAR-6982", 3130, 100);
    };
    Combine("Phase_7_comb")
    {
     R_Date("HAR-6980", 2650, 80);
     R_Date("HAR-6981", 2630, 70);
    };
    Boundary("Potterne_end");
   };
  };
  Difference("Potterne_1016", "BRAMS-1590", "HAR-6982");
  Difference("Potterne_2747", "BRAMS-1587", "BRAMS-1582");
  Difference("Potterne_2776", "BRAMS-1582", "BRAMS-1587");
  Difference("Potterne_2033", "BRAMS-1298", "Phase_7_comb");
 };
```

Figure S334. OxCal script for the Potterne Curation sequence.

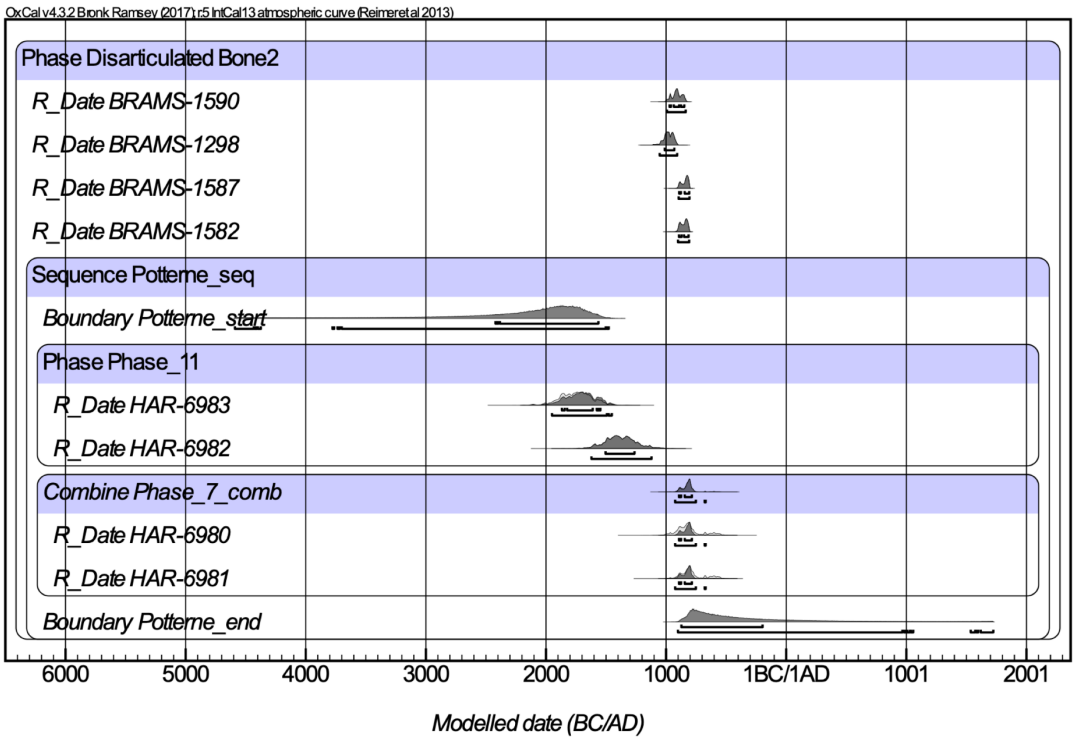

Figure S35. Potterne Curation sequence.

South Dumpton Down

Burial 15 and 16 from South Dumpton Down comprised double burial of complete articulated skeletons in a grave outside a ring ditch (Perkins 1995). Burial 15 was accompanied by the disarticulated mandible of a third human individual. We radiocarbon dated the disarticulated human mandible and the articulated human skeleton Burial 15. Combination of the dates using the Combine function in OxCal assuming the dates related to the same event produced good agreement indices and passed the X^2 test (df=1 T=0.804(5% 3.841)). These two dates were compared against one another to produced Differences in OxCal and Intervals in BChron. We generated modelled Differences by comparing the dates in a Sequence model assuming that the disarticulated mandible was older than the articulated burial.

Stanton St. Bernard

We obtained radiocarbon dates from 3 disarticulated cranial fragments (100004, 200004 and 00003) recovered from the Stanton St. Bernard midden. We had no datable material to produce comparative dates, and in any case, stratigraphic relationships between contexts at this site were fairly insecure (Dave McOmish, *pers. comm.*). We therefore compared the

radiocarbon dates against a calendrical date range for the midden inferred by associated pottery typologies (800–700 BC; Dave McOmish, *pers. comm*). We could not use the Combine function in this model, as it was possible that the cranial bones came from quite different contexts. Therefore, we put all radiocarbon dates and the calendrical date range from the pottery typology into a Phase assuming all the dates reflected a continuous horizon of activity. The Phase model produced good agreement indices. We compared the radiocarbon dates from each disarticulated human bone against the calendrical date range generated from the pottery typology to produce Differences in Oxcal. Modelled Differences were produced by comparing these dates in a Sequence model assuming that the cranial fragments were older than the pottery. To produce Intervals in BChron, we combined radiocarbon determinations from each disarticulated human bone against a simulated radiocarbon determination generated from the pottery typology range using R_Simulate in OxCal.

Striplands Farm F.2

We radiocarbon a cremated human bone from a cremation inhumation and a burnt (but not calcined) faunal bone that had both been recovered from the same context in pit on a settlement and (F.2; Evans *et al*. 2011). The weight of the cremation suggested that it did not represent the remains of a complete individual. Combination of the two dates using the Combine function in OxCal produced poor agreement indices and failed the X^2 test because the cremated human bone was too old (df=1 T=4.202(5% 3.8)). We compared these two dates to produce Differences in OxCal and Intervals in BChron. We produced modelled Differences by comparing dates in a Sequence model assuming the cremated human bone was older than the associated faunal bone.

Traigh Bahn Cist 1

We analysed radiocarbon dates that had been obtained previously from two human skeletons deposited in Traigh Bahn Cist 1 (Ritchie *et al*. 1983). The deposit comprised a complete articulated skeleton covered by the partial disarticulated remains of a second individual. Combination of the dates from these two individuals using the Combine function in OxCal assuming the dates reflect the same event produced poor agreement indices and failed the X^2 test as the date from the partial disarticulated deposit was anomalously old (df=1 T=5.172(5% 3.8)). We produced Differences in OxCal and Intervals in BChron by comparing

these two dates. We produced modelled Differences by comparing dates in a Sequence model assuming that the disarticulated skeleton was older than the articulated remains.

Trelowthas

The Trelowthas Cist 5 consisted of a stone cist containing a range of cremation deposits representing multiple individuals (Jacky Nowakowski, Cornish Archaeology Unit, *pers. comm.*). One of the cremations was found underneath the foundation stone of the cist and represented the earliest deposit stratigraphically. This cist had then been filled with cremated bones from multiple individuals, possibly in several events. A cinerary urn holding the cremated remains of at least two individuals was inserted into this accumulated deposit of cremations. We radiocarbon dated cremated human bone from the foundation deposit, two cremated human bones from discrete individuals in the main deposit and a cremated human bone from each of the individuals from the later urn. We constructed a chronological Sequence model based on these stratigraphic relationships (Figures S37–S38). The chronological model produced poor agreement indices. This was because the cremated bones from the urn were anomalously older than those from the deposit they were inserted into. We compared the dates of the cremated bones from the urn against the Boundary calculated for the end of the deposit of loose cremated bones to produce Differences in OxCal (Figure S39–S40). Modelled Differences were produced by comparing these dates in an alternative sequence assuming the cremated bones from the urn were older than the deposit they were inserted into. We compared the dates from the urned cremated bones against one of the dates from the unurned cremated bones to produce Intervals in BChron.

```
Plot()
 {
  Sequence("Cist 5")
  {
   Boundary("Cist 5_start");
   R_Date("BRAMS-1292", 3344, 24);
   Phase("Lower_spit_3")
   {
    Boundary("Lower_spit_3_start");
    R_Date("BRAMS-1288", 3318, 24);
    R_Date("BRAMS-1289", 3306, 24);
    Boundary("Lower_spit_3_end");
   };
   Combine("Vessel")
   {
    R_Date("BRAMS-1290", 3388, 24);
    R_Date("BRAMS-1291", 3341, 24);
   };
   Boundary("Cist_5_End");
  };
  Difference("Trelowthas Diff Vessel_5_3419_spit1d", "BRAMS-1290",
"Lower_spit_3_end");
  Difference("Trelowthas Diff Vessel_5_3419", "BRAMS-1291", "Lower_spit_3_end");
 };
```

Figure S36. OxCal script for the Trelowthas cist Phase model.

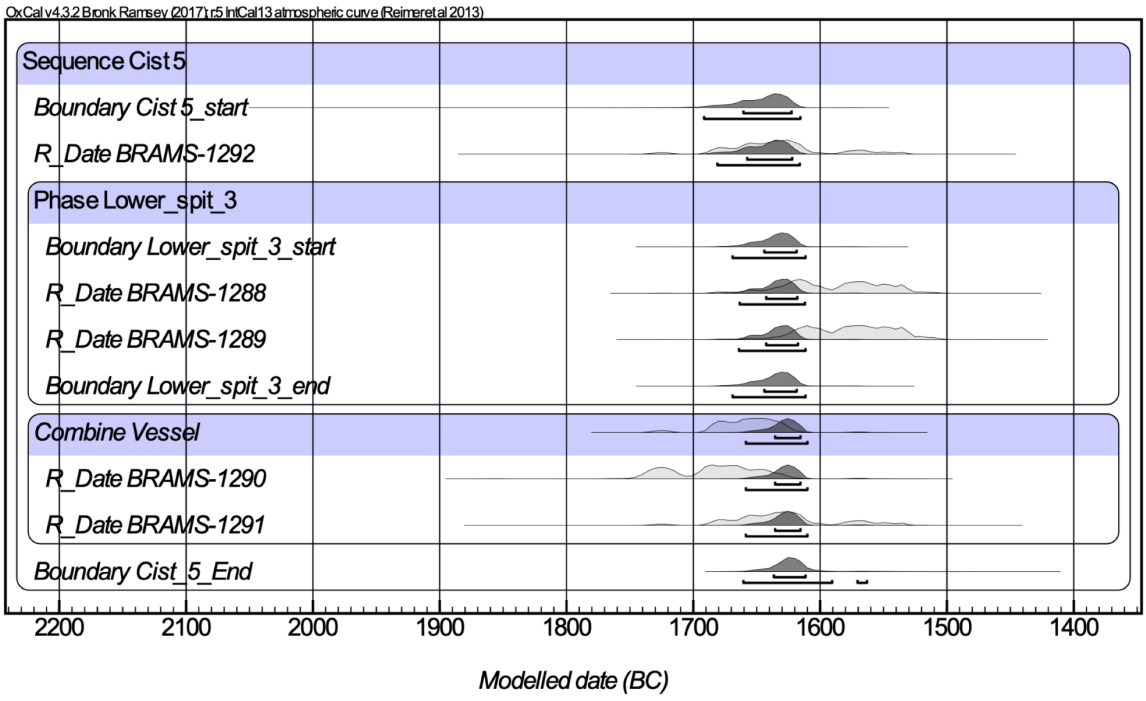

Figure S37. Trelowthas cist Phase model.

```
Plot()
 {
  Sequence("Cist 5")
  {
   Boundary("Cist 5_start");
   Phase("Earlier Phase")
   {
    R_Date("BRAMS-1292", 3344, 24);
    Combine("Vessel")
    {
     R_Date("BRAMS-1290", 3388, 24);
     R_Date("BRAMS-1291", 3341, 24);
    };
   };
   Phase("Lower_spit_3")
   {
    Boundary("Lower_spit_3_start");
    R_Date("BRAMS-1288", 3318, 24);
    R_Date("BRAMS-1289", 3306, 24);
    Boundary("Lower_spit_3_end");
   };
   Boundary("Cist_5_End");
  };
  Difference("Trelowthas Diff Vessel_5_3419_spit1d", "BRAMS-1290",
"Lower_spit_3_end");
  Difference("Trelowthas Diff Vessel_5_3419", "BRAMS-1291", "Lower_spit_3_end");
  Difference("Trelowthas Diff Vessel_5_3419_spit1d", "BRAMS-1290", "BRAMS-1289");
  Difference("Trelowthas Diff Vessel_5_3419", "BRAMS-1291", "BRAMS-1289");
 };
```

Figure S38. OxCal script for the Trelowthas Cist Curation sequence.

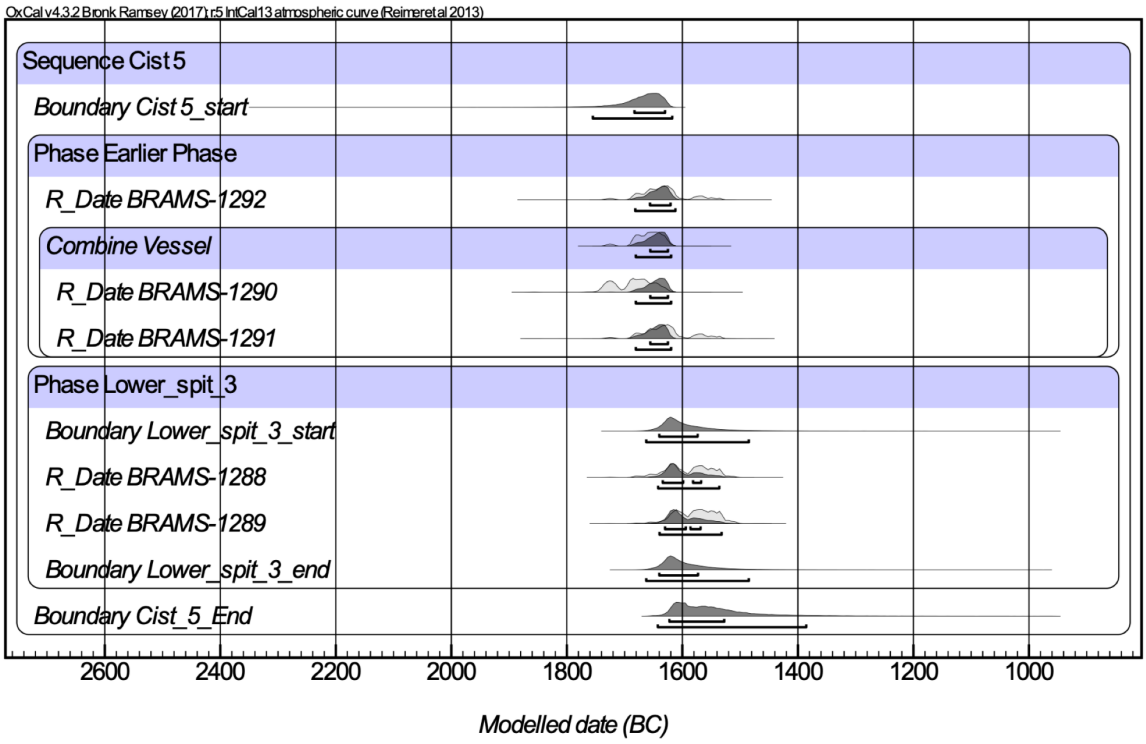

Figure S39. Trelowthas cist Curation sequence.

West Cotton

We did not generate any new radiocarbon dates for West Cotton but explored models for radiocarbon dates obtain from the site previously (Harding & Healy 2011). The authors had already recognised that disarticulated bones found accompanying complete articulated human skeletons in contexts F.3390 and F.131 were anomalously old. We used the chronological model developed in Harding and Healy (2011), but put the dates for F.3390 and F.131 into a Combine function, assuming they related to the same event, rather than including them as part of Phases which assumed they belong to the same broad horizon of activity (Figures S41–S42). The model using Combine would not run because of the large disparity in dates from F.3390, which showed poor agreement and failed the X^2 test. However, the Combine model for the dates from F.131 also showed poor agreement indices and failed the X^2 test. We tested dates of the disarticulated bones against ones from the articulated skeletons to generate Differences in OxCal and Intervals in BChron (Figures S43–S44). We produced modelled Differences by comparing dates in a Sequence model which assumed the disarticulated human bones were older than the articulated burials they accompanied.

```
Plot()
 {
  Phase("Bronze Age barrows")
  {
   Sequence("Barrow 1")
   {
    Phase("F30426")
    {
     Last("Barrow_1");
     R_Date("UB-3148", 3681, 47);
     R_Date("OxA-7902", 3775, 45);
     R_Date("OxA-4067", 4100, 80);
     R_Date("OxA-2087", 3810, 80);
     R_Date("OxA-2086", 3810, 80);
     R_Date("OxA-2084", 3610, 110);
     R_Date("OxA-2085", 4040, 80);
    };
    Phase("post-cattle")
    {
     R_Date("UB-3147", 3504, 38);
    };
   };
   Sequence("Barrow 3")
   {
    Phase("charcoal in ditch")
    {
     R_Date("OxA-7903", 3650, 45);
     R_Date("OxA-7949", 3610, 40);
    };
    R_Date("OxA-3051", 3590, 70);
   };
   Sequence("Barrow 4")
   {
    R_Date("OxA-3052", 3450, 70);
    After("Plank in mound")
    {
     R_Date("OxA-3053", 3530, 70);
    };
   };
   Phase("Barrow 5")
   {
    R_Date("OxA-3054", 4460, 70);
    R_Combine("291-55243")
    {
     R_Date("OxA-7950", 3625, 40);
     R_Date("OxA-3120", 3680, 100);
    };
   };
   Sequence("Barrow 6")
   {
    Boundary("Barrow 6 start");
    Combine("F.3390 comb")
    {
     R_Date("UB-3310", 4500, 33);
     R_Date("UB-3311", 3608, 41);
    };
    Phase("cremations in ditch")
    {
     R_Date("OxA-7866", 3610, 40);
     R_Date("UB-3315", 3347, 54);
    };
    Boundary("Barrow 6 end");
   };
   Phase("Barrow 9")
   {
    R_Combine("skeleton 747")
    {
     R_Date("OxA-5543", 3645, 45);
     R_Date("OxA-5542", 3750, 55);
    };
    R_Combine("skeleton 732")
    {
     R_Date("OxA-5547", 3495, 40);
     R_Date("OxA-5548", 3500, 70);
    };
    R_Date("BM-2866", 3610, 50);
    R_Combine("skeleton 737")
    {
     R_Date("OxA-5546", 3615, 45);
     R_Date("OxA-5545", 3690, 40);
    };
   };
   Phase("inhumations in long barrow")
   {
    Combine("F.131 comb")
    {
     R_Date("OxA-5550", 3730, 45);
     R_Date("BM-2833", 3450, 45);
    };
    R_Date("OxA-5549", 3665, 45);
   };
  };
 };
```

Figure S41. OxCal script for the West Cotton Phase model.

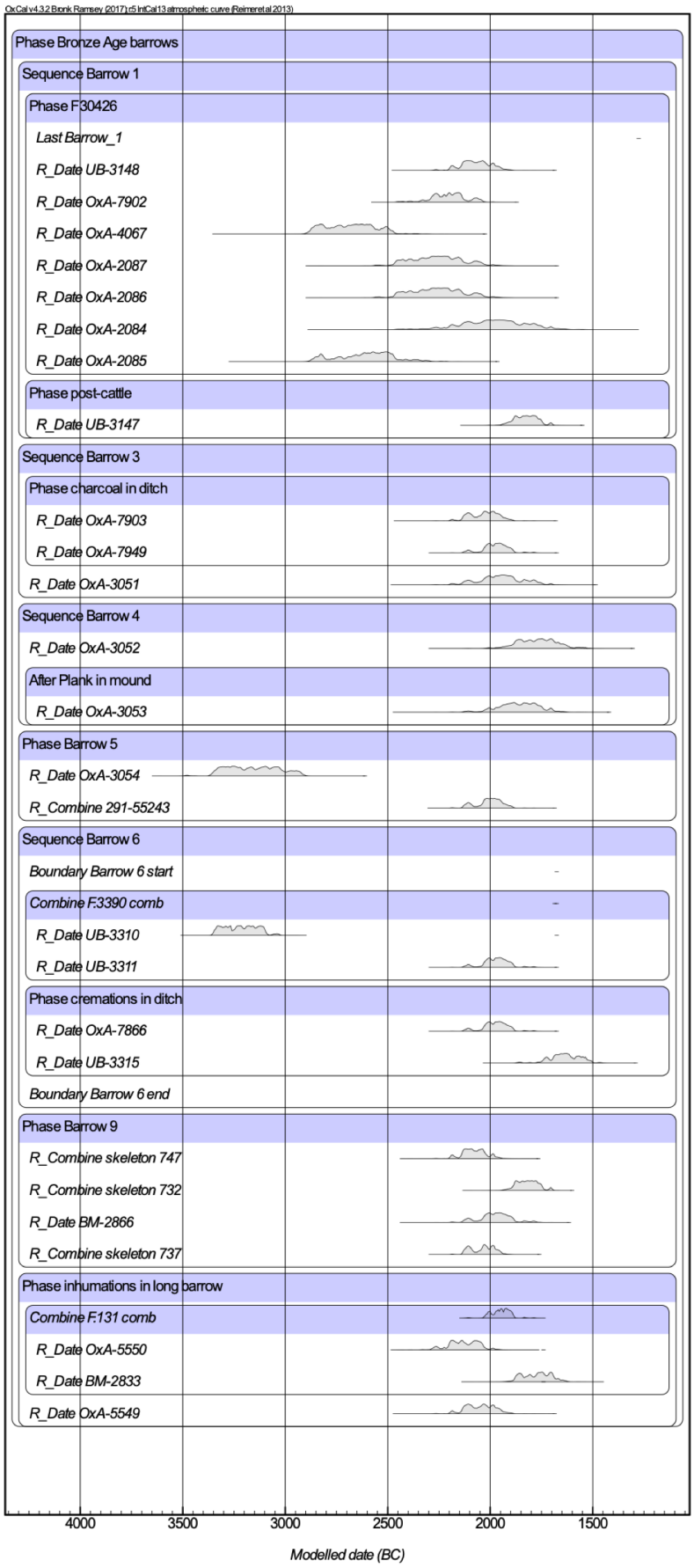

Figure S42. West Cotton Phase model.

```
Plot()
 {
  Phase("Bronze Age barrows")
  {
   Sequence("Barrow 1")
   {
    Phase("F30426")
    {
     Last("Barrow_1");
     R_Date("UB-3148", 3681, 47);
     R_Date("OxA-7902", 3775, 45);
     R_Date("OxA-4067", 4100, 80);
     R_Date("OxA-2087", 3810, 80);
     R_Date("OxA-2086", 3810, 80);
     R_Date("OxA-2084", 3610, 110);
     R_Date("OxA-2085", 4040, 80);
    };
    Phase("post-cattle")
    {
     R_Date("UB-3147", 3504, 38);
    };
   };
   Sequence("Barrow 3")
   {
    Phase("charcoal in ditch")
    {
     R_Date("OxA-7903", 3650, 45);
     R_Date("OxA-7949", 3610, 40);
    };
    R_Date("OxA-3051", 3590, 70);
   };
   Sequence("Barrow 4")
   {
    R_Date("OxA-3052", 3450, 70);
    After("Plank in mound")
    {
     R_Date("OxA-3053", 3530, 70);
    };
   };
   Phase("Barrow 5")
   {
    R_Date("OxA-3054", 4460, 70);
    R_Combine("291-55243")
    {
     R_Date("OxA-7950", 3625, 40);
     R_Date("OxA-3120", 3680, 100);
    };
   };
   Sequence("Barrow 6")
   {
    Boundary("Barrow 6 start");
    Sequence("F.3390 seq")
    {
     R_Date("UB-3310", 4500, 33);
     R_Date("UB-3311", 3608, 41);
    };
    Phase("cremations in ditch")
    {
     R_Date("OxA-7866", 3610, 40);
     R_Date("UB-3315", 3347, 54);
    };
    Boundary("Barrow 6 end");
   };
   Phase("Barrow 9")
   {
    R_Combine("skeleton 747")
    {
     R_Date("OxA-5543", 3645, 45);
     R_Date("OxA-5542", 3750, 55);
    };
    R_Combine("skeleton 732")
    {
     R_Date("OxA-5547", 3495, 40);
     R_Date("OxA-5548", 3500, 70);
    };
    R_Date("BM-2866", 3610, 50);
    R_Combine("skeleton 737")
    {
     R_Date("OxA-5546", 3615, 45);
     R_Date("OxA-5545", 3690, 40);
    };
   };
   Phase("inhumations in long barrow")
   {
    Sequence("F.131 Seq")
    {
     R_Date("OxA-5550", 3730, 45);
     R_Date("BM-2833", 3450, 45);
    };
    R_Date("OxA-5549", 3665, 45);
   };
  };
  Difference("F.3990 diff", "UB-3310", "UB-3311");
  Difference("F.131_diff", "OxA-5550", "BM-2833");
 };
```

Figure S40. OxCal script for the West Cotton Curation sequence.

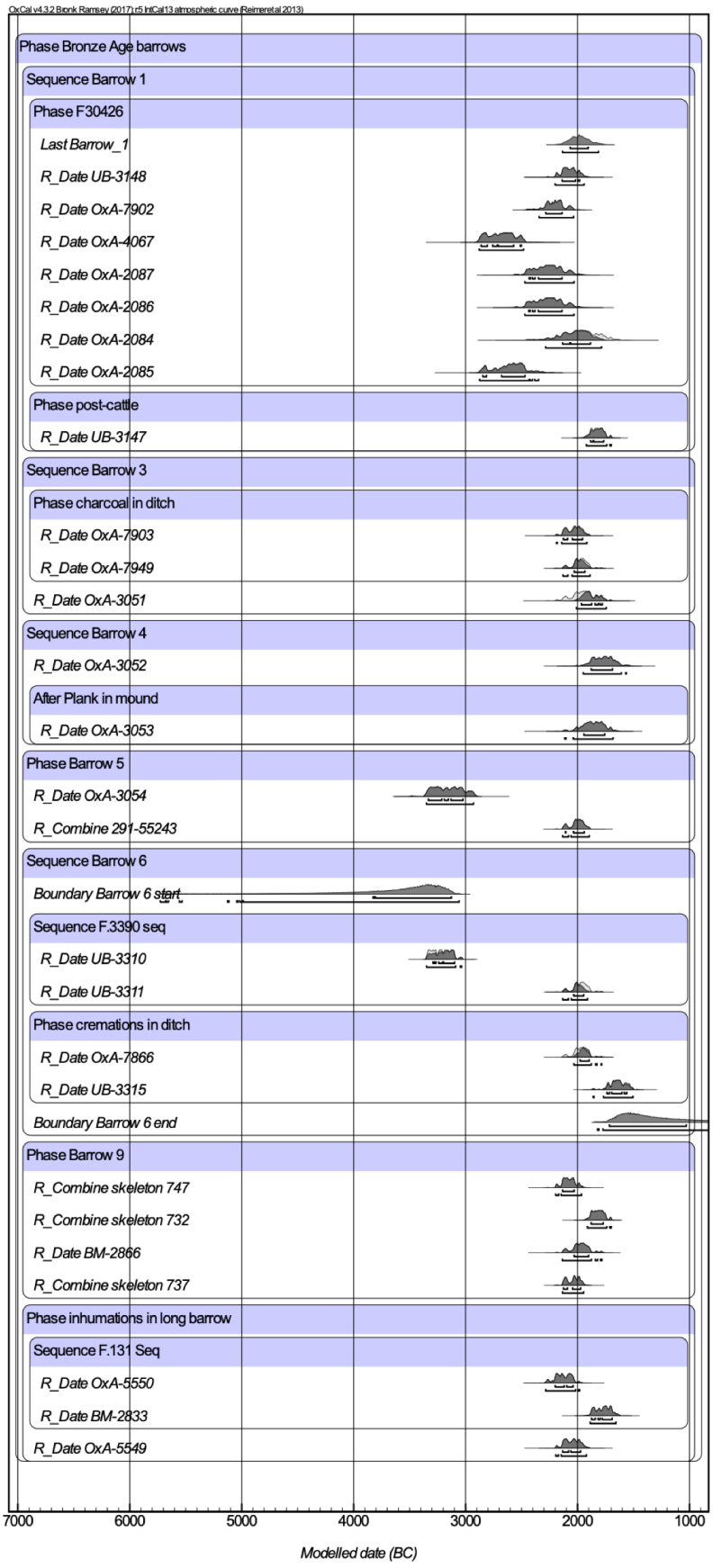

Figure S41. West Cotton Curation sequence.

Whitton Hill

Whitton Hill comprised a deposit of cremated bone in a pit representing the mixed remains of at least 24 individuals (Gamble & Fowler 2013). There was no archaeological evidence that the pit had been revisited, indicating that all individuals had been deposited in a single event. However, the weight of the deposit could not account for all 24 individuals, suggesting that only part of at least some of the individuals represented in this assemblage had been deposited. One cremated human bone from this deposit had been radiocarbon dated previously. We radiocarbon dated two more cremated bones representing discrete individuals, bringing the number of dated individuals up to three. Combination of dates using the Combine function in OxCal assuming they related to the same event produced poor agreement indices and failed the X^2 test (df=2 T=7.381(5% 6.0)). Two of the cremated bones were anomalously older than the third. We compared the dates of each of the older cremated bones against the date from the younger bone to generate Differences in OxCal and Intervals in BChron. We generated modelled Differences by comparing dates in a Sequence model assuming that cremated bones were different ages.

Wicken (Dimmock's Quote Quarry) 1254

We radiocarbon dated a disarticulated cranial bone and two disarticulated faunal bones from the same context (1254) of a natural hollow (Gilmour 2014). Combination of the three dates using the Combine function in OxCal assuming that all dates relate to the same event produced poor agreement indices and failed the X^2 test (df=2 T=7.364(5% 6.0)). However, this was because the radiocarbon date from one of the disarticulated faunal bones was anomalously old. Either this date was erroneous, or this faunal bone was already old when it was deposited and may have been curated itself. We reran the Combine function without the anomalous faunal bone. This model produced good agreement indices and passed the X^2 test (df=1 T=1.608(5% 3.841)). We produced Differences in OxCal and Intervals in BChron by comparing the date from the disarticulated human bone to the date from the younger faunal bone. We generated modelled Differences by comparing dates in a Sequence model assuming that the disarticulated human cranium is older than the associated faunal remains.

Wilsford G.58

We radiocarbon dated a disarticulated human femur that had been worked into a musical instrument, which accompanied the complete articulated skeleton that was the primary burial in the Wilsford G.58 round barrow (Woodward & Hunter 2015). The articulated human

skeleton was reburied and there is no surviving dateable material from the grave. Therefore, we compared the date from the musical instrument against a calendrical date range inferred by the typology of artefacts found in the same grave (C_Date, 1950–1700 BC; Woodward & Hunter 2015). Combination of these two dates using the Combine function in OxCal assuming the dates relate to the same event produced good agreement indices and passed the X^2 test (df=1 T=1.253(5% 3.841)). We produced Differences in OxCal by comparing the date from the musical instrument against the calendrical date inferred from the artefacts. We produced a radiocarbon determination for the calendrical dates inferred from the artefact typology using R_Simulate. We compared this simulated date against the date from the musical instrument in BChron to generate an Interval in BChron. We produced modelled Differences by comparing dates in a Sequence model assuming that the worked femur was older than the associated materials.

Section 2. Variability in Detecting patterns of Curation through time.

Fluctuations in the radiocarbon calibration curve means that the interval between the death of an individual and the deposition of their bones required for the two to show up as significantly different varies through time. We simulated five sets of radiocarbon determinations from calendrical dates in 10-year intervals to assess for how long a bone would have to have been curated at different points in the Bronze Age before its radiocarbon date would fail a X^2 test (Supplementary Figure S45; Table S4). We tested each interval against all preceding dates using the Combine function in OxCal 4.3 and the IntCal13 curve (Ward & Wilson 1978; Bronk Ramsey 2009a; Reimer *et al.* 2013). The vagaries of the calibration curve mean that there are time points at which a sample may fail the X^2 test at one interval, but pass at an older interval. This produces two thresholds; one where certain intervals will begin to fail variably and another where they fail invariably (Figure 2). The results suggest in the Copper and Early Bronze Age where the calibration curve is flatter, bones would have had to have been around two centuries old before they failed the X^2 test. In the Late Bronze Age where the calibration curve is steeper, bones would only have to have been curated for a few decades to fail. This sets limits to what we would expect to be able to find and say and suggests that it may be difficult to tell whether disarticulated unburnt bones/deposits of burnt bone had been buried soon after death, or curated for short periods of time (i.e. a few decades) based on X^2 tests alone.

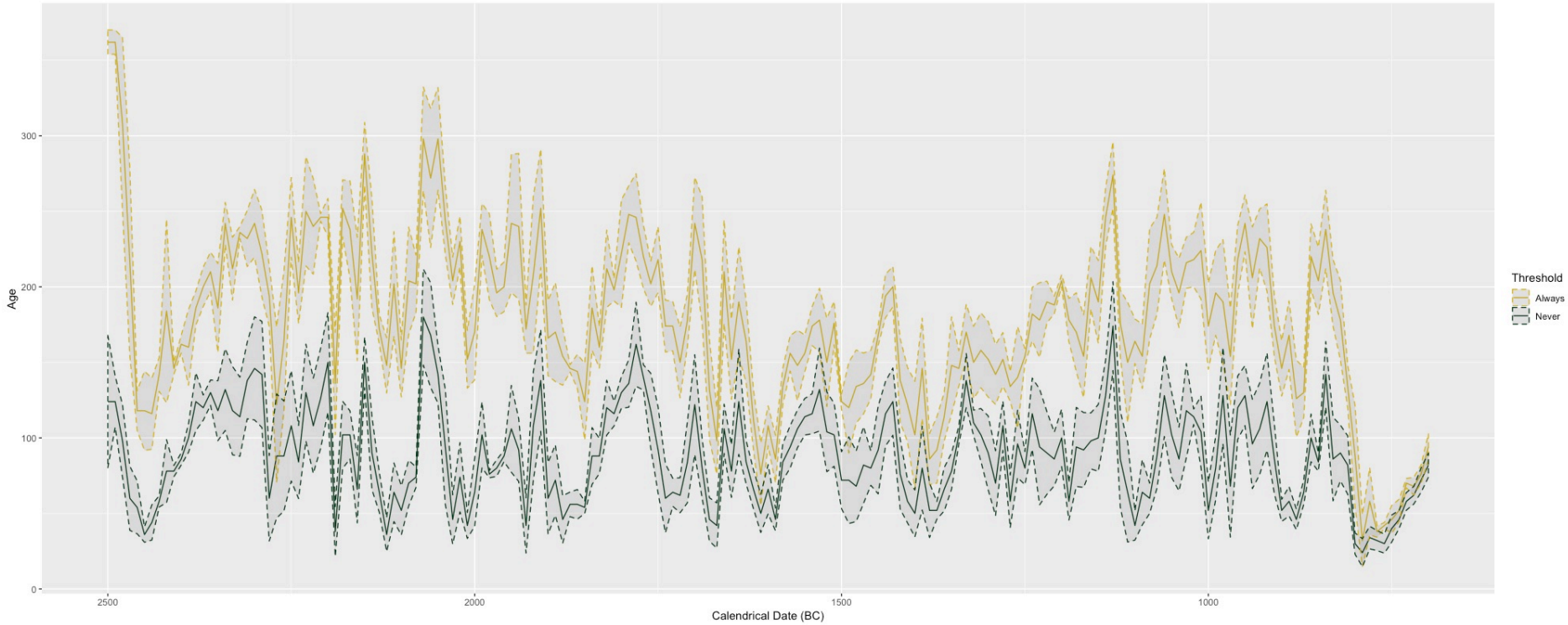

Figure S45: Line graph showing the variability in the age a sample would have to be before it would show up as significantly old through the Bronze Age using simulated ages and the Combine function in OxCal. The green line ('Never') displays the mean and standard error for ages coming back as invariably significant, and the yellow line ('Always') shows the same figures for the threshold where ages are always significant.

Section 3. Micro-CT methods.

Scans were performed on long bone and cranial vault fragments that had been sampled for radiocarbon dating. Bone samples were embedded in Oasis floral foam (Oasis Floral products) within a plastic beaker. X-ray micro-CT scans were performed at the Image Analysis Centre (IAC) at the Natural History Museum, London using a Nikon Metrology HMX ST 255 (Nikon Metrology, Tring, UK) micro-CT scanner fitted with a 0.1mm Cu filter. All scans were carried out at 150mA with a molybdenum target and 3142 projections were taken over a 360 rotation with no frame averaging. Samples were CT scanned at exposures of 708 ms with accelerating voltages of 180-200Kv. Three-dimensional volumes were reconstructed from the micro-CT scans with CT Pro (Nikon metrology, Tring, UK) using a modified Feldkamp back-projection algorithm (Feldkamp *et al*. 1984). The 3D data were rendered using VG Studio Max (Volume Graphics, Heidelberg, Germany) to analyse the quality of the scans and produce three- dimensional visualisations. We also used VG Studio Max to produce stacks of two-dimensional transverse cross-sections, equivalent to transverse bone thin sections. Scans were performed on long bone and cranial vault fragments. All fragments included a cross-section of bone extending from the periosteal to the endosteal surface. Bioerosion can vary intra-skeletally; however there is no apparent variation in levels of attack between cranial and long bones examined here (Jans *et al.* 2004; Hollund *et al.* 2015). There is no variation in the pattern and extent of bioerosion through bone volumes, consistent with previous micro-CT studies of bone bioerosion indicating that virtual slices are representative of whole samples (Dal Sasso *et al.* 2014; Booth *et al.* 2016).

References

ANNIS, R. *et al*. 1997. An unusual group of early Bronze Age burials from Windmill Fields, Ingleby Barwick, Stockton-on-Tees. Unpublished report, Tees Archaeology.

APPLEBY, G. 2005. Bradley Fen: the metalwork in context. University of Cambridge Unpublished Master's dissertation, University of Cambridge

BOOTH, T.J., A.T. CHAMBERLAIN. & M. PARKER PEARSON. 2015. Mummification in Bronze Age Britain *Antiquity* 89: 1155–73. https://doi.org/10.15184/aqy.2015.111

BOOTH, T.J., R.C. REDFERN & R.L. GOWLAND. 2016. Immaculate conceptions: micro-CT analysis of diagenesis in Romano-British infant skeletons *Journal of Archaeological Science* 74: 124–34. https://doi.org/10.1016/j.jas.2016.08.007

BRONK RAMSEY, C. 2009a. Bayesian analysis of radiocarbon dates. *Radiocarbon* 51: 337–60. https://doi.org/10.1017/S0033822200033865

– 2009b. Dealing with outliers and offsets in radiocarbon dating. *Radiocarbon* 51: 1023–45. https://doi.org/10.1017/S0033822200034093

BRUNNING, R. 1997. Two Bronze Age wooden structures in the Somerset Moors. *Archaeology in the Severn Estuary* 8: 5–8.

DAL SASSO, G., L. MARITAN, D. USAI, I. ANGELINI & G. ARTIOLI. 2014. Bone diagenesis at the micro-scale: bone alteration patterns during multiple burial phases at Al Khiday (Khartoum, Sudan) between the Early Holocene and the II century AD. *Palaeogeography, Palaeoclimatology, Palaeoecology* 416: 30–42. https://doi.org/10.1016/j.palaeo.2014.06.034

DUNWELL, A., *et al*. 2007. Cist burials and an Iron Age settlement at Dryburn Bridge, Innerwick, East Lothian. Scottish Archaeological Internet Reports 24. https://doi.org/10.5284/1017938

EVANS, C. & M. VANDER LINDEN. 2009. The Over Narrows: archaeological investigations in Hanson's Needingworth Quarry. Godwin Ridge East-Central. Unpublished report, Cambridge Archaeological Unit.

EVANS, C., R. PATTEN, M. BRUDENELL & M. TAYLOR. 2011. An inland Bronze Age: excavations at Striplands Farm, West Longstanton. *Proceedings of the Cambridge Antiquarian Society* 100: 7–45.

FELDKAMP, L.A., L.C. DAVIS & J.W. KRESS. 1984. Practical cone-beam algorithm. *Journal of the Optical Society of America* 1: 612e619. https://doi.org/10.1364/JOSAA.1.000612

FITZPATRICK, A.P. 2013. *The Amesbury Archer and the Boscombe Bowmen: Early Bell Beaker burials at Boscombe Down, Amesbury, Wiltshire*. Salisbury: Wessex Archaeology.

GAMBLE, M. & C. FOWLER. 2013. A re-assessment of human skeletal remains in Tyne and Wear Museums: results and implications for interpreting Early Bronze Age burials from Northeast England and beyond. *Archaeologia Aeliana* 42: 47–80.

GIBSON, D. & M. KNIGHT. 2006. Bradley Fen Excavations 2001–2004, Whittlesey, Cambridgeshire. Unpublished report, Cambridge Archaeological Unit.

GILMOUR, N. 2014. Early Neolithic to medieval archaeology at Dimmock's Cote Quarry, Wicken, Cambridgeshire, archaeological investigations from 1992 to 2011. Unpublished report, Oxford Archaeology East.

HARDING, J. & F. HEALY. 2011. *The Raunds area project: a Neolithic and Bronze Age landscape in Northamptonshire*. Swindon: English Heritage.

HASLETT, J. & A. PARNELL. 2008. A simple monotone process with application to radiocarbon-dated depth chronologies. *Journal of the Royal Statistical Society: Series C (Applied Statistics)* 57: 399–418. https://doi.org/10.1111/j.1467-9876.2008.00623.x

HOLLUND, H.I., N. ARTS, M.M.E. JANS & H. KARS. 2015. Are teeth better? Histological characterization of diagenesis in archaeological bone-tooth pairs and a discussion of the consequences for archaeometric sample selection and analyses. *International Journal of Osteoarchaeology* 25: 901–11.

JANS, M.M.E., C.M. NIELSEN-MARSH, C.I. SMITH, M.J. COLLINS & H. KARS. 2004. Characterisation of microbial attack on archaeological bone. *Journal of Archaeological Science* 31: 87–95.

LAWSON, A., M. J. ALLEN & A. BAYLISS. 2000. Radiocarbon dating, in A. J. Lawson (ed.) *Potterne 1982–5: animal husbandry in later prehistoric Wiltshire* (Report 17). Salisbury: Trust for Wessex Archaeology: 39–42.

LELONG, O. *et al*. 2018. Fluid identities, shifting sands: Early Bronze Age burials at Cnip Headland, Isle of Lewis. Scottish Archaeological Internet Reports 75. https://doi.org/10.9750/issn.2056-7421.2018.75

MORTIMER, R. & T. PHILLIPS. 2012. Clay Farm, Trumpington, Cambridgeshire: post-excavation assessment. Unpublished report, Oxford Archaeology East.

MCKINLEY, J.I., M. LEIVERS, J. SCHUSTER & P. MARSHALL. 2015. *Cliffs End Farm Isle of Thanet, Kent: a mortuary and ritual site of the Bronze Age, Iron Age and Anglo-Saxon period with evidence for long-distance maritime mobility*. Salisbury: Wessex Archaeology.

PARKER PEARSON, M. *et al*. 2005. Evidence for mummification in Bronze Age Britain *Antiquity* 79: 529–46. http://dx.doi.org/10.1017/s0003598x00114486

PARKER PEARSON, M., *et al*. 2007. Further evidence for mummification in Bronze Age Britain. *Antiquity* Project Gallery 81.

PATTEN, R. 2004. Bronze Age and Romano-British activity at Eye Quarry, Peterborough Phase 3. Unpublished report, Cambridge Archaeological Unit.

PERKINS, D.R.J. 1995. An assessment/research design: South Dumpton Down, Broadstairs. Unpublished report, Trust for Thanet Archaeology.

PICKSTONE, A. & R. MORTIMER. 2011. The archaeology of Brigg's Farm, Prior's Fen, Thorney, Peterborough. Unpublished report, Oxford Archaeology East.

POWELL, K., G. LAWS & L. BROWN. 2008. A Late Neolithic/Early Bronze Age enclosure and Iron Age and Romano-British settlement at Latton Lands, Wiltshire. Unpublished report, Oxford Archaeology South.

R Core Team. 2013. R: a language and environment for statistical computing. Available at https://www.r-project.org (accessed 22 May 2020).

REIMER, P.J. *et al*. 2013. IntCal13 and Marine13 radiocarbon age calibration curves 0–50 000

years cal BP. *Radiocarbon* 55: 1869–87. https://doi.org/10.2458/azu_js_rc.55.16947

RITCHIE, J., J. STEVENSON, D.A. LUNT, C.R. WICKHAM-JONES & A. YOUNG. 1982. Cists at Traigh Bhan, Islay, Argyll. *Proceedings of the Society of Antiquaries of Scotland* 112: 550–59.

SMITH, A., K. POWELL & P. BOOTH. 2010. Evolution of a farming community in the Upper Thames Valley, excavation of a prehistoric, Roman and post-Roman landscape at Cotswold Community, Gloucestershire and Wiltshire Volume 2: the finds and environmental reports. Unpublished report, Oxford Archaeology South.

SMITH, M.J., M.J. ALLEN, G. DELBARRE, T. BOOTH, P. CHEETHAM, L. BAILEY, F. O'MALLEY, M. PARKER PEARSON & M. GREEN. 2016. Holding on to the past: southern British evidence for mummification and retention of the dead in the Chalcolithic and Bronze Age. *Journal of Archaeological Science: Reports* 10: 744–56. https://doi.org/10.1016/j.jasrep.2016.05.034

WOODWARD, A. & J. HUNTER. 2015. *Ritual in Early Bronze Age grave goods: an examination of ritual and dress equipment from Chalcolithic and Early Bronze Age graves in England*. Oxford: Oxbow.